TRIBHUVAN UNIVERSITY
INSTITUTE OF ENGINEERING
PULCHOWK CAMPUS

FLOW VISUALIZATION IN CENTRIFUGAL PUMP IMPELLER USING PARTICLE IMAGE VELOCIMETRY (PIV)

By:
ABLE KHANAL(077BME003)
ANUNAYA GARTAULA (077BME004)
BENZEENA DHAKAL (077BME006)
NRIPESH DHUNGANA (077BME024)

A PROJECT REPORT
SUBMITTED TO THE DEPARTMENT OF MECHANICAL AND AEROSPACE ENGINEERING IN PARTIAL FULFILLMENT OF THE REQUIREMENT FOR THE DEGREE OF BACHELOR'S IN MECHANICAL ENGINEERING

DEPARTMENT OF MECHANICAL AND AEROSPACE ENGINEERING
LALITPUR, NEPAL

APRIL 2025

COPYRIGHT

LETTER OF APPROVAL

TRIBHUVAN UNIVERSITY
INSTITUTE OF ENGINEERING
CENTRAL CAMPUS PULCHOWK
DEPARTMENT OF MECHANICAL AND AEROSPACE ENGINEERING

The undersigned certify that they have read, and recommended to the Institute of Engineering for acceptance, a project report entitled "FLOW VISUALIZATION OF CENTRIFUGAL PUMP IMPELLER USING PARTICLE IMAGE VELOCIMETRY (PIV)" submitted by Able Khanal, Anunaya Gartaula, Benzeena Dhakal and Nripesh Dhungana in partial fulfillment of the requirements for the degree of Bachelor of Mechanical Engineering.

Supervisor, Dr. Rajendra Shrestha
Professor
Department of Mechanical and Aerospace Engineering
Institute of Engineering, Pulchowk Campus

Supervisor, Kamal Darlami
Assistant Professor
Department of Mechanical and Aerospace Engineering
Institute of Engineering, Pulchowk Campus

External Examiner, Salim Maharjan
Assistant Professor
Himalaya Engineering College

Head of Department, Dr. Sudip Bhattarai
Assistant Professor
Department of Mechanical and Aerospace Engineering
Institute of Engineering, Pulchowk Campus

Date: 2025/04/30

ABSTRACT

Centrifugal pumps are widely utilized in industrial fluid transport; however, performance challenges such as vortex formation and distorted velocity profiles can significantly impact their efficiency and reliability. This study employs Particle Image Velocimetry (PIV) to investigate the flow dynamics within the impeller and volute of a centrifugal pump. A transparent centrifugal pump was designed and fabricated and the flow in its impeller and volute was analyzed using the PIV technique. Cross-correlation analysis was performed with the PIVlab software to obtain velocity field measurements. This study provides insight into the application of PIV at low pump speeds and visualizes the vortices formed at the beginning of the rotation of the impeller. The findings contribute to understanding the flow dynamics in centrifugal pumps and to enhancing its scope for use in other engineering applications.

KEYWORDS: PIV, Centrifugal Pump, PIVlab, cross-correlation, flow visualization

ACKNOWLEDGEMENT

We would like to express our sincere gratitude to the **Department of Mechanical and Aerospace Engineering, IOE Pulchowk Campus**, for providing us with the opportunity to undertake this final year project. This project has been an incredible journey, allowing us to delve into the field of Particle Image Velocimetry (PIV) for flow visualization.

Our heartfelt thanks go to our supervisors, **Prof. Dr. Rajendra Shrestha** and **Asst. Prof. Kamal Darlami**, whose constant support, guidance, and encouragement have been a source of motivation throughout this project. Asst. Prof. Kamal Darlami not only provided us with the workspace at the Incubation, Innovation, and Entrepreneurship Center (IIEC) but also offered continuous advice and insights during our meetings, helping us navigate through challenges and stay focused on our goals. We are deeply thankful to Fab Lab Nepal, a small-scale, open-access workshop operating under ImpactHUB Kathmandu that enables individuals to design, prototype, and fabricate almost anything using digital fabrication tools and technologies. We express our sincere gratitude to **Er. Pallab Shrestha** and **Er. Shashank Dewan**, for their continuous guidance, support, and valuable feedback, and for allowing us to use CNC routing and laser cutting machines for the fabrication of pump components.
Additionally, we would like to extend our deepest appreciation to **Rodolfo Marcilli Perissinotto**, Ph.D., Research Scientist at CEPETRO/UNICAMP, for his thoughtful support during the design phase of the prototype and for sharing his expertise on PIV. His guidance was crucial in shaping our project, and we are truly grateful for his willingness to help.
Lastly, we want to thank our seniors, teachers, friends, and parents for always encouraging and supporting us. Their advice, feedback, and belief in us made a big difference and helped us complete this project. We truly appreciate everything they've done for us.

Authors:

- 077BME003 (ABLE KHANAL)
- 077BME004 (ANUNAYA GARTAULA)
- 077BME006 (BENZEENA DHAKAL)
- 077BME024 (NRIPESH DHUNGANA)

TABLE OF CONTENTS

COPYRIGHT i

LETTER OF APPROVAL ii

ABSTRACT iii

ACKNOWLEDGEMENT iv

TABLE OF CONTENTS v

LIST OF TABLES viii

LIST OF FIGURES x

LIST OF SYMBOLS xi

LIST OF ABBREVIATIONS xii

1 INTRODUCTION 1
- 1.1 Background . . . 1
- 1.2 Problem Statement . . . 1
- 1.3 Objectives . . . 2
  - 1.3.1 Main Objectives . . . 2
  - 1.3.2 Specific Objectives . . . 2
- 1.4 Application . . . 2
  - 1.4.1 Pump Performance Optimization . . . 2
  - 1.4.2 Experimental Validation for Pump Design . . . 2
  - 1.4.3 Research and Academic Use . . . 3
- 1.5 Feasibility Analysis . . . 3
  - 1.5.1 Economic Feasibility . . . 3
  - 1.5.2 Technical Feasibility . . . 3
  - 1.5.3 Operational Feasibility . . . 3
- 1.6 System Requirements . . . 3
  - 1.6.1 Hardware Requirements . . . 3
  - 1.6.2 Software Requirements . . . 4

2 LITERATURE REVIEW 5
- 2.1 Theoretical Background . . . 5
  - 2.1.1 Centrifugal Pump Operation and velocity triangles . . . 5
  - 2.1.2 Net head developed by the pump . . . 7
  - 2.1.3 Efficiencies . . . 8
  - 2.1.4 Volumetric efficiency (η_v) . . . 8
  - 2.1.5 Losses in the centrifugal pump . . . 9
  - 2.1.6 Specific Speed . . . 10
- 2.2 Particle Image Velocimetry (PIV) . . . 11
  - 2.2.1 Seeding Particles . . . 12

2.2.2 Laser and Optics . . . 13
2.2.3 Image Pre-Processing . . . 13
2.2.4 Cross-Correlation . . . 13
2.2.5 Validation and Interpolation . . . 15
2.3 Papers Reviewed . . . 15

3 METHODOLOGY **17**
3.1 Design Phase . . . 18
3.1.1 Design Considerations . . . 18
3.1.2 Initial parameters Used . . . 18
3.1.3 Impeller . . . 19
3.1.4 Impeller blade . . . 20
3.1.5 Mid Section Volute . . . 20
3.1.6 Front Acrylic Plane . . . 22
3.1.7 Rear Acrylic Plane . . . 22
3.1.8 Pump Shaft . . . 23
3.1.9 Pump Assembly . . . 23
3.2 CAD Model . . . 23
3.3 Fabrication Phase . . . 25
3.3.1 Impeller Fabrication . . . 25
3.3.2 Volute Casing Fabrication . . . 25
3.3.3 Shaft Assembly . . . 26
3.3.4 Experimental Setup . . . 26
3.4 Simulation Phase . . . 26
3.5 Validation phase . . . 32
3.5.1 Theoretical Pump Head Curve . . . 32
3.5.2 Head-capacity Relations . . . 33
3.5.3 Actual Pump Head Curve . . . 35
3.6 Experimental Phase . . . 38
3.6.1 PIV Setup . . . 38
3.6.2 PIV Validation . . . 39
3.6.3 Flow Visualization of Centrifugal Pump Impeller using PIV . . . 41

4 RESULT AND DISCUSSION **43**
4.1 Result . . . 43
4.1.1 Flow Visualization in centrifugal pump impeller and volute . . . 43
4.2 Limitations . . . 45
4.3 Problems Faced . . . 45
4.4 Budget Analysis . . . 47
4.5 Discussion . . . 47

5 CONCLUSION AND FUTURE ENHANCEMENT **48**
5.1 Conclusion . . . 48
5.2 Scope for Future Enhancement . . . 48

REFERENCES **49**

APPENDIX **50**

A Fabrication **51**

B CODES **52**
B.1 Arduino Code: Flow sensor 52

C CODES **53**
C.1 Matlab Code to Generate Theoretical Head Curve 53
C.2 Matlab Code to Generate Actual Pump Head Curve 55

D CAD drawing of Pump Components **58**

LIST OF TABLES

2.1 Specific Speed Classification of Centrifugal Pumps[1] 10
2.2 Specification of seeding particles 12

3.1 Pump Specifications at BEP 19
3.2 Impeller known parameters 20
3.3 Specific Speed Calculations[2] 20
3.4 Average Fluid Velocity in the Volute 21
3.5 Pump Performance Data 27
3.6 Theoretical Pump performance characteristics at different RPM 36
3.7 Pump performance at different RPM 38

4.1 Budget Analysis 47

LIST OF FIGURES

2.1 Forces and Velocities in an impeller [1] . . . 6
2.2 Inlet Velocity Triangle [1] . . . 6
2.3 Outlet Velocity Triangle[1] . . . 6
2.4 Performance curves for three stages of a pump . . . 7
2.5 Variation of Specific Speed[1] . . . 11
2.6 Illustrative scheme of a conventional PIV system . . . 12
2.7 Direct Cross Correlation [3] . . . 14
2.8 Cross-Correlation via FFT [4] . . . 14

3.1 Methodology Flow Chart . . . 17
3.2 PIV Process Flowchart . . . 18
3.3 Impeller Parameter[5] . . . 19
3.4 Volute Constants[1] . . . 21
3.5 CAD models of pump components: (a) impeller and (b) volute . . . 24
3.6 Acrylic plane CAD models showing front and rear views . . . 24
3.7 Pump Assembly . . . 24
3.8 Fabricated Acrylic Parts(Before Assembling) . . . 25
3.9 Schematic Diagram of Experimental PIV Setup . . . 26
3.10 Contour of Total Pressure (pt) at 50% span . . . 28
3.11 Contour of Static Pressure (ps) at 50% span . . . 29
3.12 Velocity Vector at 20% span . . . 30
3.13 Velocity Vector at 50% span . . . 31
3.14 Velocity Vector at 80% span . . . 31
3.15 Velocity streamlines at Blade Trailing Edge . . . 32
3.16 Difference between actual and theoretical curve . . . 33
3.17 Theoretical Pump Head Curve . . . 34
3.18 Actual Pump Head Curve . . . 37
3.19 Fabricated Experimental Setup . . . 39
3.20 PIV Setup for Flow Visualization . . . 39
3.21 Digital Cameras used for PIV . . . 40
3.22 100mW Laser and Cylindrical Lens used for Planar Illumination[6] . . . 40
3.23 Flow Channel with Sinusoidal waveform Structure . . . 41
3.24 Velocity and vorticity fields at a certain time in the sine wave . . . 42

4.1 Mean velocity vectors of flow at 30rpm in clockwise direction showing variation in vorticity . . . 43
4.2 Variation in vorticity from impeller to the volute . . . 44
4.3 Variation in vorticity and streamlines to visualize it . . . 44
4.4 Variation in vorticity and streamlines to visualize it . . . 45
4.5 Post processed images of pump running at 10 rpm . . . 46
4.6 Variation in vorticity from impeller to the volute in impeller running at 10rpm anti-clockwise . . . 46

A.1 Fabrication process components: (a) acrylic parts before assembly, (b) UV adhesive, (c) volute fabrication, and (d) shaft fabrication . . . 51

D.1 Front Plane 58
D.2 Mid Section Volute 58
D.3 Rear Acrylic Plane 59
D.4 Impeller Shroud 59
D.5 Impeller Blade 60
D.6 Pump Shaft 60

LIST OF SYMBOLS

ω	Angular velocity of shaft
H	Pump Head
N	Pump Speed
p	Pressure
ρ	Density
g	Acceleration due to gravity
V	Average velocity of fluid flow
z	Elevation
Q	Volume flow rate
T	Torque
u	peripheral velocity of impeller
w	Relative velocity of flow
c	absolute velocity of flow
r	Radial distance
e_h	Hydraulic Efficiency
e_v	Volumetric Efficiency
e_m	Mechanical Efficiency
e	Total or gross Efficiency
θ	Angular distance
z	Meridional distance
v	Fluid velocity
U	Local fluid velocity
X	Particle position
t	Time

LIST OF ABBREVIATIONS

3D Three Dimensional

BEP Best Efficiency Point

BHP Brake Horse Power

CLAHE Contrast Limited Adaptive Histogram Equalization

CAD Computer Aided Drawing

CCD Charge-Coupled Device

CFD Computational Fluid Dynamics

CMOS Complementary Metal Oxide Semiconductor

DFT Discrete Fourier Transform

ESP Electrical Submersible Pump

FFT Fast Fourier Transform

HD High Definition

LASER Light Amplification by Stimulated Emission of Radiation

LDV Laser Doppler Velocimetry

PIV Particle Image Velocimetry

PLA Polyactic Acid

PTV Particle Tracking Velocimetry

SST Shear Stress Transport

CHAPTER 1
INTRODUCTION

1.1 Background

Centrifugal pumps are indispensable components in a wide range of industrial applications, from water supply systems and agricultural irrigation to petroleum refineries, chemical processing plants, and power generation facilities. These pumps operate on the principle of imparting energy to fluids, facilitating their efficient transport through pipelines and systems. The operational efficiency and reliability of centrifugal pumps are primarily governed by two critical components: the impeller and the casing. The impeller is responsible for imparting kinetic energy to the fluid by accelerating it outward through rotational motion. A casing is a spiral-shaped housing that surrounds the impeller.It gradually increases in cross-sectional area, which helps convert velocity into pressure as the fluid moves outward. Together, these components play a pivotal role in determining pump performance, making their design and functionality central to the pump's efficiency.

In industrial operations, centrifugal pumps often encounter complex flow phenomena such as distorted velocity profiles, pressure gradients, and vortex formation. These phenomena can lead to reduced efficiency, increased wear, and operational reliability issues, particularly under conditions that deviate from the pump's Best Efficiency Point (BEP). Understanding the internal fluid dynamics within the impeller and volute is critical for addressing these challenges. Insights into flow behavior are essential not only for optimizing pump performance but also for diagnosing and resolving operational issues, ensuring long-term reliability and reduced maintenance costs.

Flow visualization techniques have emerged as invaluable tools for studying the intricate dynamics of fluid systems within centrifugal pumps. These techniques enable researchers and engineers to observe, measure, and analyze flow characteristics under a variety of operating conditions. Among the many methods available, Particle Image Velocimetry (PIV) stands out as a highly advanced optical measurement technique, offering unparalleled accuracy and detail.

PIV involves seeding the fluid with tracer particles that faithfully follow the flow. These particles are illuminated by a laser sheet, and their motion is captured sequentially by cameras. By analyzing the displacement of particles between images, PIV generates high-resolution velocity field data. This method is non-intrusive, preserving the natural behavior of the fluid while providing precise and instantaneous measurements of complex flow characteristics such as turbulence, vortices, and velocity gradients.

In the context of centrifugal pumps, PIV has proven to be particularly valuable for understanding the intricate flow dynamics within the impeller and volute. It allows for the direct visualization of phenomena such as vortex formation, recirculation zones, and pressure gradients—factors that significantly influence pump performance.

1.2 Problem Statement

Centrifugal pumps often experience flow issues such as distorted velocity profiles, pressure gradients, and vortex formation, which reduce their performance and reliability. These complex flow dynamics

are challenging to analyze using traditional methods, making experimental investigation essential for a better understanding. This research aims to use Particle Image Velocimetry (PIV) to experimentally analyze the flow inside a centrifugal pump impeller, providing accurate velocity field data for improved flow visualization and performance evaluation.

1.3 Objectives

1.3.1 Main Objectives

The main objective of this project is to perform the flow visualization within the impeller and volute of a centrifugal pump using Particle Image Velocimetry (PIV).

1.3.2 Specific Objectives

The specific objectives of the project are as mentioned below:

- To design and fabricate a transparent centrifugal pump prototype by replicating an existing impeller and casing, enabling clear and detailed visualization of internal flow dynamics.
- To develop a fully functional PIV setup for analyzing flow behavior within the centrifugal pump impeller.
- To conduct PIV experiments on centrifugal pump prototype to investigate the flow characteristics and velocity fields.
- To analyze the experimental data obtained from the PIV setup to extract meaningful insights about the flow behavior.
- To carry out the simulation of the impeller of a centrifugal pump to identify the performance parameters of the pump.

1.4 Application

1.4.1 Pump Performance Optimization

- Provides detailed insights into internal flow behavior, enabling design improvements for enhanced efficiency and reliability.
- Helps reduce energy losses by identifying flow disturbances such as vortices and recirculation zones.

1.4.2 Experimental Validation for Pump Design

- Supports manufacturers in validating new impeller and volute designs through direct flow visualization.
- Enhances accuracy in predicting real-world pump performance.

1.4.3 Research and Academic Use

- Serves as a valuable resource for fluid mechanics research, particularly in experimental flow analysis.
- Provides an educational platform for engineering students and researchers studying pump dynamics.

1.5 Feasibility Analysis

The development of a Particle Image Velocimetry (PIV) setup and a transparent pump prototype depends on several factors, including economic, technical, and operational feasibility. A detailed feasibility analysis is presented below.

1.5.1 Economic Feasibility

The estimated cost for fabricating the transparent pump prototype, modifying the PIV setup, and conducting experiments is approximately Rs. 30800. This includes expenses for Acrylic sheets, UV Glue, fabrication of pump prototype, PIV setup, RPM controller, pressure gauge, shaft fabrication and so on. Additionally, the availability of major components—such as a continuous plane sheet laser and high-speed camera—at the Department of Mechanical and Aerospace Engineering significantly reduces costs. Based on this assessment, the research is economically feasible.

1.5.2 Technical Feasibility

The availability of software for the design and analysis of components, combined with the local availability of a 3D printer for fabricating test specimens, ensures that the research is technically feasible. Additionally, the presence of a PIV setup for analyzing flow characteristics further validates the technical viability of the research. The necessary seeding particles are also available in the Department of Mechanical and Aerospace Engineering at IOE Pulchowk Campus.

1.5.3 Operational Feasibility

The design and fabrication of the transparent pump prototype, along with the use of PIV for research analysis, relies on fundamental principles of PIV, making it straightforward to implement. The availability of specialized software like PIVlab and openPIV for post-processing images ensures efficient and accurate data analysis. The presence of skilled personnel and necessary equipment within the department further enhances the operational feasibility of the project.

1.6 System Requirements

1.6.1 Hardware Requirements

1. Chronos 2.1-HD High speed Camera
2. 100 mw point Class IIIB Laser (400-500 nm)
3. Hollow glass spheres as seeding particles
4. Acrylic Sheets

5. Electric Motor with variable RPM controller
6. Pipes and fittings
7. Pressure Gauge
8. Flow sensor
9. Valves
10. Reservoir
11. Tachometer

1.6.2 Software Requirements

1. DS SOLIDWORKS
2. ANSYS
3. MATLAB with installed PIVlab
4. Arduino IDE

CHAPTER 2
LITERATURE REVIEW

2.1 Theoretical Background

2.1.1 Centrifugal Pump Operation and velocity triangles

A centrifugal pump operates on the principle that a rotating fluid is pushed away from the central axis due to centrifugal force, creating a pressure head that lifts the fluid to a higher level. The operation begins with priming, where the suction pipe, casing, and part of the delivery pipe are filled with liquid to eliminate air pockets. The impeller is then set in motion by an electric motor, generating a vacuum at the impeller's eye, which draws fluid into the pump. As the impeller reaches normal speed, the delivery valve is opened, allowing the fluid to be continuously sucked from the sump and propelled through the vanes, where its velocity and pressure increase. The fluid exits the impeller, passes through the casing, and is discharged through the delivery pipe at the required height. This process continues as long as the impeller rotates and liquid is supplied, with the delivery valve closed before stopping to prevent backflow.

A centrifugal pump consists of four main components: the impeller, casing, suction pipe, and delivery pipe. The impeller, mounted on a rotating shaft, comes in three types—closed, semi-open, and open—depending on the presence of cover plates, with applications ranging from clean water to debris-filled liquids. The casing, an airtight chamber, surrounds the impeller and guides fluid flow, converting kinetic energy into pressure energy. It can be a volute casing, vortex casing, or casing with guide blades, each enhancing efficiency differently. The suction pipe connects the sump to the impeller's eye, fitted with a strainer to block debris and a foot valve to prevent backflow. The delivery pipe directs the pumped fluid to its destination, with a regulating valve to control flow.

A study of the several component velocities of flow through an impeller is best carried out graphically by means of velocity vectors. The shape of such vector diagrams is triangular, and they are called velocity triangles. They can be drawn for any point of the flow path through the impeller, but usually, attention is focused on the entrance and discharge part of the impeller vanes, and the velocity triangles are called the entrance and discharge triangles. It is necessary to distinguish between absolute and relative velocities. The relative velocity of flow is considered relative to the impeller. The absolute velocity of flow is taken with respect to the firm casing and is always equal to the vectorial sum of the relative velocity and the peripheral velocity of the impeller. Any point on the impeller will describe a circle about the shaft axis and will have a peripheral velocity U1 and U2.

$$u1 = \frac{\pi * N * d1}{60}$$

$$u2 = \frac{\pi * N * d2}{60}$$

where d1 and d2 are the diameters of the circle at the inlet and outlet of the impeller.
The following notation is adopted:
u -peripheral velocity of impeller
w -relative velocity of flow
c -absolute velocity of flow
Subscript 1 refers to the entrance; subscript 2 to the discharge. Tangential components of relative and absolute velocities are given another subscript, u. Components of the absolute velocity normal to the

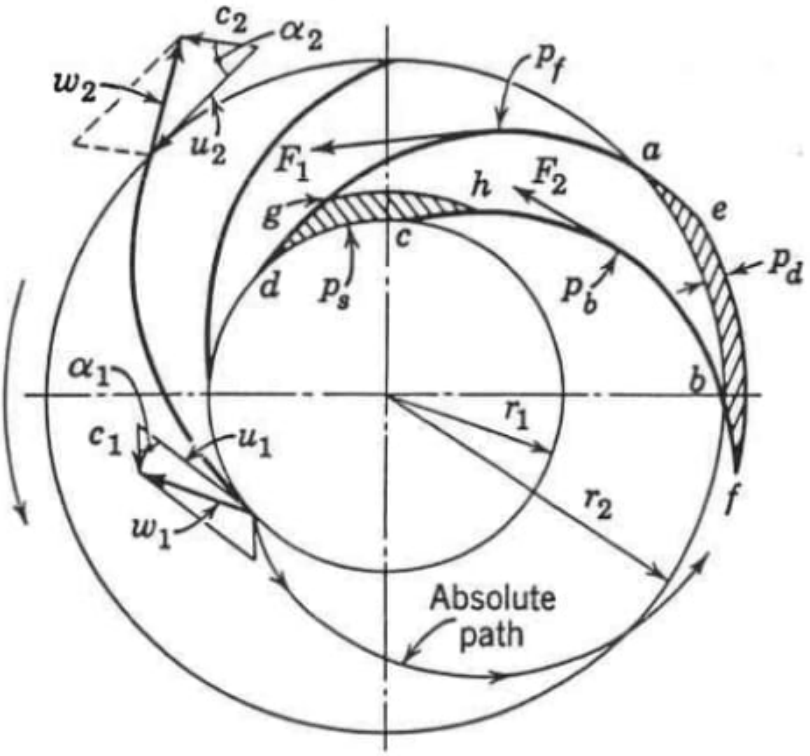

Figure 2.1: Forces and Velocities in an impeller [1]

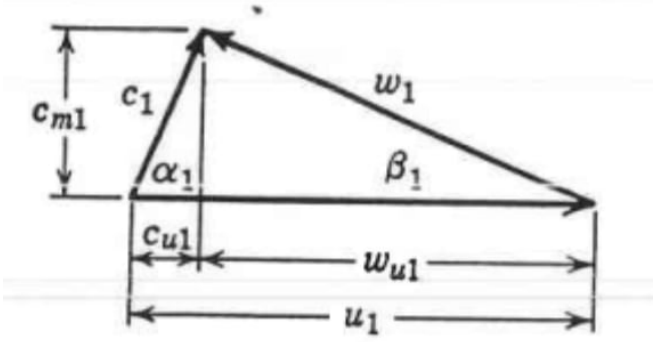

Figure 2.2: Inlet Velocity Triangle [1]

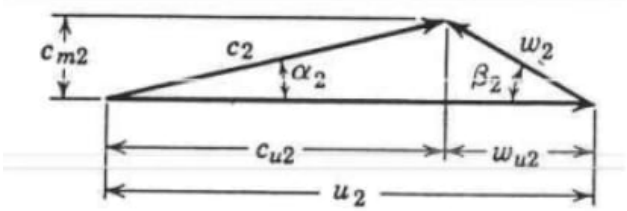

Figure 2.3: Outlet Velocity Triangle[1]

peripheral velocity are designated as cm1 and cm2 for entrance and discharge diagrams. This component is radial in a radial impeller and axial in an axial impeller. It will be referred to, in general, as meridional and will have the subscript m. Unless specifically stated, all velocities are considered average velocities for the section normal to the general direction of flow at a specified point. This is one of the approximations made for theoretical studies and practical design, which is not true in practice.

An expression for the theoretical head of a centrifugal pump is obtained by applying the principle of angular momentum to the mass of liquid going through the impeller passages. This principle states that the time rate of change of angular momentum of a body with respect to the axis of rotation is equal to the torque of the resultant force on the body with respect to the same axis.

$$H_i = \frac{u_2 v_{u2} - u_1 v_{u1}}{g}$$

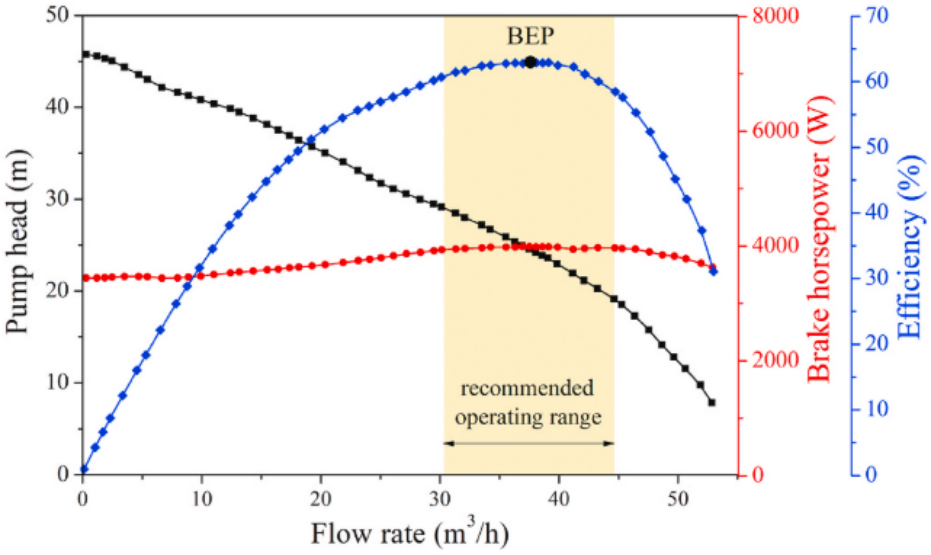

Figure 2.4: Performance curves for three stages of a Schlumberger GN 5200 pump at N=3500rev/min [7][8]

Fig. 2.4 shows the efficiency curve of a centrifugal pump with a low-viscosity fluid. The curve has the maximum value at the Best Efficiency Point, denoted by BEP. The efficiency of pumps depends on fluid properties and flow characteristics and is adversely affected by the presence of viscous liquids and/or gases.

2.1.2 Net head developed by the pump

The total inlet head to the pump is calculated as:

$$\frac{p_1}{\rho g} + \frac{V_1^2}{2g} + z_1$$

The total outlet head of the pump is calculated as :

$$\frac{p_2}{\rho g} + \frac{V_2^2}{2g} + z_2$$

Here $p_1$and p_2 are the pressures and V_1 and V_2 are the velocities in suction and delivery pipes, respectively. Similarly, $z_1$and z_2 are the datum positions of inlet and outlet.

The total head developed by the pump is given by the expression(H):

$$\left[\frac{p_2 - p_1}{\rho g} + \frac{V_2^2 - V_1^2}{2g} + Z_2 - Z_1\right]$$

The head developed H is termed the manometric head. It is also expressed as H_{mano}.

2.1.3 Efficiencies

2.1.3.1 Manometric efficiency (η_{mano})

The ratio of the manometric head developed by the pump to the head imparted by the impeller to the liquid is known as manometric efficiency:

$$\eta_{mano} = \frac{\text{Manometric Head}}{\text{Head imparted by impeller to liquid}}$$

$$\eta_{mano} = \frac{H_{mano}}{\left(\frac{V_{w2}u_2}{g}\right)} = \frac{gH_{mano}}{V_{w2}u_2}$$

2.1.4 Volumetric efficiency (η_v)

The ratio of the quantity of liquid discharged per second from the pump to the quantity passing per second through the impeller is known as volumetric efficiency:

$$\eta_v = \frac{\text{Liquid discharged per second from the pump}}{\text{Quantity of liquid passing per second through the impeller}}$$

$$\eta_v = \frac{Q}{Q+q}$$

Where:

- Q = Actual liquid discharge at the pump outlet per second
- q = Leakage of liquid per second from the impeller (through the clearances between the impeller and casing)

2.1.4.1 Mechanical efficiency (η_m)

The ratio of the power delivered by the impeller to the liquid to the power input to the pump shaft is known as mechanical efficiency:

$$\eta_m = \frac{\text{Power delivered by the impeller to the liquid}}{\text{Power input to the pump shaft}}$$

$$\eta_m = \frac{w(Q+q)(V_{w2}u_2/g)}{P}$$

2.1.4.2 Overall efficiency (η_0)

The ratio of power output of the pump to the power input to the pump is known as overall efficiency:

$$\eta_0 = \frac{\text{Power output of the pump}}{\text{Power input to the pump}}$$

$$\eta_0 = \frac{wQH_{mano}}{P}$$

$$\eta_0 = \eta_{mano} \times \eta_v \times \eta_m$$

2.1.5 Losses in the centrifugal pump

Not all the energy supplied to a centrifugal pump is turned into useful work. Some energy is always lost inside the pump. These losses can be grouped into three main types: **hydraulic losses**, **mechanical losses**, and **leakage losses**. Knowing about these helps us make pumps work better and last longer.

2.1.5.1 Hydraulic Losses

These losses happen because the water (or any liquid) rubs against the pump parts and changes direction quickly inside the pump. There are two main reasons for this:

- **Shock and Eddy Losses:** When water enters or leaves the spinning part (impeller), it sometimes doesn't follow the blades smoothly. This sudden change causes swirling and turbulence, wasting energy.
- **Friction Losses:** As water moves through the pump's pipes and passages, it rubs against the walls. The rougher or longer the path, the more energy is lost as heat.

Hydraulic losses are usually bigger when the pump is not working at its best speed or flow. Good pump design and smooth surfaces help reduce these losses.

2.1.5.2 Mechanical Losses

Mechanical losses come from moving parts inside the pump:

- **Disc Friction Losses:** The spinning impeller drags against the water in the small gaps between the impeller and the casing, causing some energy loss.
- **Bearing and Seal Friction:** The shaft spins on bearings and passes through seals, which also create friction and use up some energy.

These losses mostly depend on how fast the pump is spinning and the quality of its parts. They don't change much with flow rate, but they matter more when the pump is running slowly.

2.1.5.3 Leakage (Volumetric) Losses

Some of the water leaks back inside the pump instead of going out the discharge pipe:

- **Clearance Gaps:** Small gaps between the impeller and the pump casing let some water slip back from high-pressure to low-pressure areas.
- **Balancing Holes:** Some pumps have holes to balance forces on the impeller, but these also let water leak internally.

Leakage losses get worse as the pump wears out. Keeping clearances tight and doing regular maintenance helps keep these losses low.

All these losses add up and lower the pump's efficiency. Most good centrifugal pumps are about **60–85% efficient**. By choosing the right pump, running it near its best operating point, and doing regular maintenance, we can keep these losses as low as possible and save energy.

Understanding and reducing these losses helps pumps work better and last longer.

2.1.6 Specific Speed

The specific speed (N_s) of a centrifugal pump is defined as the speed of a geometrically similar pump which would deliver a unit quantity (one cubic meter of liquid per second) against a unit head (one meter). The required expression of specific speed for the pump is:

$$N_s = \frac{N\sqrt{Q}}{H^{3/2}}$$

The **specific speed in metric units** (n_q) and **US units** (N_s) are related by [1]:

$$N_s = 51.64 \times n_q$$

- n_q uses metric units: flow in m^3/s, head in meters, speed in rpm.
- N_s uses US customary units: flow in gallons per minute (gpm), head in feet, speed in rpm.

2.1.6.1 Interpretation of Specific Speed Ranges

Table 3.2 classifies centrifugal pumps based on their specific speed (N_s), which is a fundamental design parameter that correlates impeller geometry with performance characteristics.

Table 2.1: Specific Speed Classification of Centrifugal Pumps[1]

Pump Type	**Specific Speed (n_q)**	**Specific Speed (N_s)**
Slow Speed	10–30	500–1500
Medium Speed	30–50	1500–2600
High Speed	50–80	2600–5700
Mixed Flow	80–160	5700–8300
Axial Flow	160–500	8300–26000

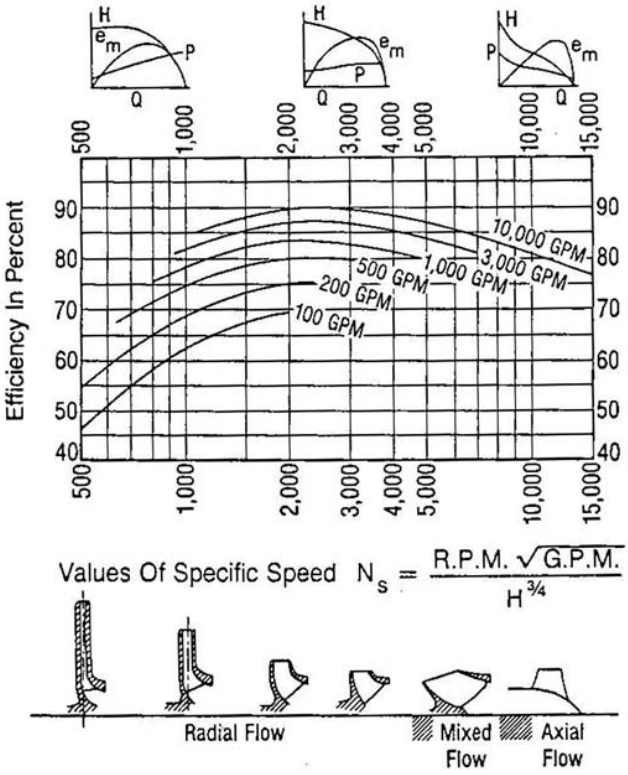

Figure 2.5: Variation of Specific Speed[1]

2.2 Particle Image Velocimetry (PIV)

Particle Image Velocimetry involves recording the position of a group of particles (X) in consecutive instants of time (t); then algorithms determine the displacement of these particles(ΔX) for a known interval of time(Δt):

$$U = \frac{\Delta X(X,t)}{\Delta t}$$

A two-dimensional PIV method involved the following elements: a laser generator, a digital camera, an electronic circuit responsible for synchronizing each pulse emitted by the laser with each image captured by the camera, a set of mirrors and lenses to convert the light beam into a thin sheet that illuminated the plane of flow [8].

The dashed lines in the figure above highlight the image processing with a cross correlation routine which calculates the displacement of tracer particles (X) to estimate the local fluid velocity The flow is usually measured by a planar laser light sheet technique in which the light sheet is pulsed twice, and images of fine particles lying in the light sheet are recorded on a high-performance CCD or CMOS camera.

The displacement of the particle image is measured in the plane of the image and is used to determine the displacement of the particles in the flow. The most common way of measuring displacement is to divide the image plane into small interrogation spots and cross-correlate the images from the two time exposures.

Cross-correlation is a statistical technique used to measure the similarity between two signals or datasets as a function of the displacement of one relative to the other.

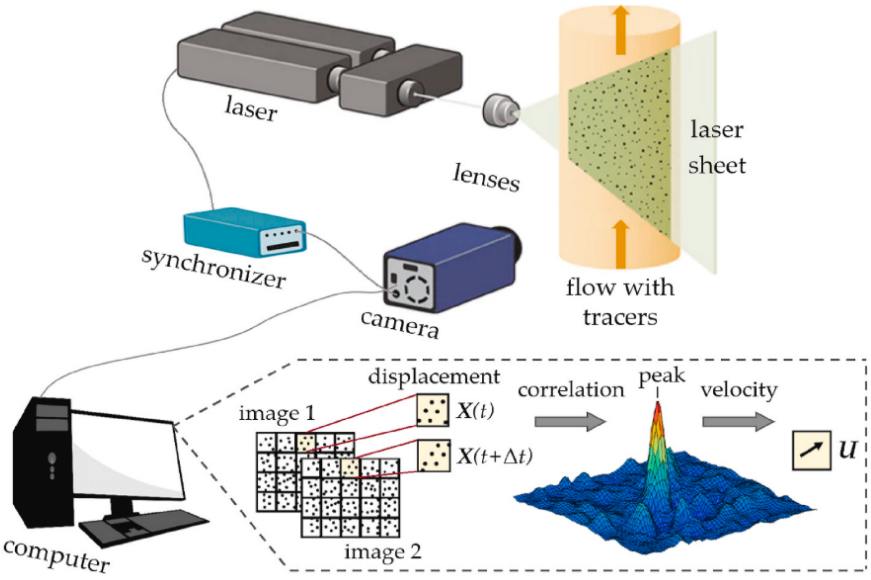

Figure 2.6: Illustrative scheme of a conventional PIV system (2D-2C PIV) used in a generic experiment [8]

2.2.1 Seeding Particles

Seeding particles are objects distinctly visible under illumination from high-intensity light sources such as lasers; these particles when inserted into fluid flows follow the motion of fluid and therefore provide indication of the nature of movement of the fluid. Following are the parameters of seeding particles to be considered for efficient Particle Image Velocimetry: Stokes number (Stk), Relaxation Time(τ_s) and Settling Time(V_T)[9].

	Polyamide Seeding Particles	Hollow Glass Spheres	Silver Coated Hollow Glass Spheres	Fluorescent Polymer Particles
Mean diameter µm	5, 20, 50	10	10	10, 30, 75
Size distribution	1 – 10 µm 5 – 35 µm 30 – 70 µm	2 – 20 µm	2 – 20µm	1 – 20 µm 20 – 40 µm 50 – 100 µm
Particle shape	non-spherical but round	spherical	spherical	spherical
Density (g/cm³)	1.03	1.1	1.4	1.5
Melting point (°C)	175	740	740	250
Material	Polyamide 12	Borosilicate glass	Borosilicate glass	Melamine resin based polyester

Table 2.2: Specifications of Seeding Particles for Use in Liquid Flows [DANTEC®] [4]

Stokes number (Stk) is a dimensionless parameter that characterizes behavior of particles in fluid flows and is mathematically the ratio of particle response time to characteristic fluid flow time. Relaxation Time (τ_s) is an indication of the response of particle to changes in fluid flow and is a function of

particle density (ρ_p) and individual particle diameter (d_p). It is desirable to select a particle with minimal relaxation time. Settling Time(V_T) is the time it takes for particles to settle in the surface of a reservoir or flow channel under the influence of gravity and it is a function of difference between particle density(ρ_p) and fluid density(ρ_f). The settling time is ideally to be as large as possible to observe uniform and even particle concentration in images[9].

2.2.2 Laser and Optics

Lasers are used in PIV because of their ability to emit monochromatic light of high energy density which can be bundled into a light sheet for planar illumination. Laser material consists of an atomic or molecular gas, semiconductor or solid material.
Nd:YAG Lasers: Neodym lasers of wavelength λ=532nm are solid state lasers used in PIV applications. Beam is generated by Nd^{3+} and YAG(Yttrium-Aluminum-Garnet) crystals are used for amplification[9].
The essential element for generation of a laser sheet is cylindrical lens; a single cylindrical lens when used with a laser of high intensity is sufficient to produce necessary planar illumination[9].

2.2.3 Image Pre-Processing

PIVLab consists of several image pre-processing tools to enhance subsequent cross-correlation computations. PIVLab provides the following pre-processing alternatives and an image can be run through none or all of them as required.

- **Contrast Limited Adaptive Histogram Equalization** : Contrast Limited Adaptive Histogram Equalization, abbreviated as CLAHE, is a tool that distributes most frequent image intensity obtained on a histogram across all data points, resulting in even distribution of low and high exposure regions[3][6].
- **High-Pass Filter:** High Pass-filter suppresses low-frequency background information generated by uneven lighting and suppresses displacement data for such low-frequency information[3][6].
- **Intensity Capping:** Uneven particle movement as a result of non-uniform fluid may cause uneven distribution of particles within interrogation window which results in inaccurate correlation counts; disproportionately bright particles also offset correlation counts and produce faulty results. Intensity Capping filter helps produce valid velocity vectors by limiting grayscale intensity[3][6].
- **Wiener2 Denoise:** It is a denoising filter that calculates local noise and corresponding signal-to-noise ratio inside a selected pixel window, and uses local filter to minimize mean-squared error[3][6].
- **Contrast Stretching:** This filter helps define minimum and maximum normalised contrast values for expanding dynamic intensity[3][6].

2.2.4 Cross-Correlation

PIV systems employ the use of Cross-Correlation of sub-images within two image sets to determine the most likely displacement of particles in the sub-images. The sub-images are called interrogation areas/windows; the entire image is divided into a number of these interrogation areas/windows with cross-correlation processes being performed such that each interrogation window generates one vector. Cross-correlation is carried out in two ways: Direct Cross Correlation(DCC) or Discrete Fourier

Transform(DFT)[3]. Direct Cross Correlation shifts a sub-image or interrogation window from pre-image over post-image and uses convolution filtering to calculate cross-correlation for different interrogation window positions[3]. This involves high computational costs for large images and also prevents the use of small interrogation windows for the same reasons.

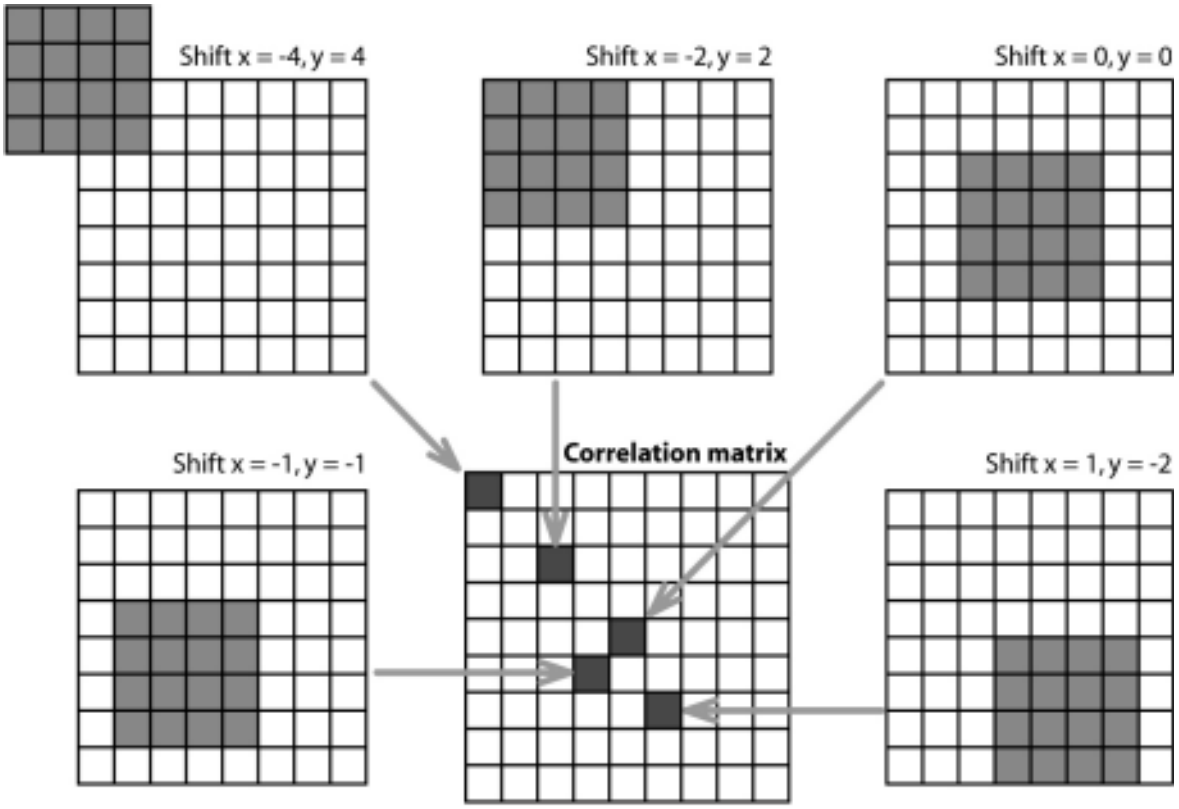

Figure 2.7: Direct Cross Correlation [3]

To minimize computational costs, Discrete Fourier Transformation of Interrogation windows is carried out which removes the need for convolution filtering and attains cross correlation values through inverse fourier transform of the product of the fourier transforms of the interrogation window and the search window. Discrete Fourier Transform is carried out via Fast Fourier Transformation(FFT) algorithm[4]. The major drawback of DFT Cross-Correlation is the drop in accuracy for low signal-to-noise ratio, requiring the use of multiple passes which increases computational costs.

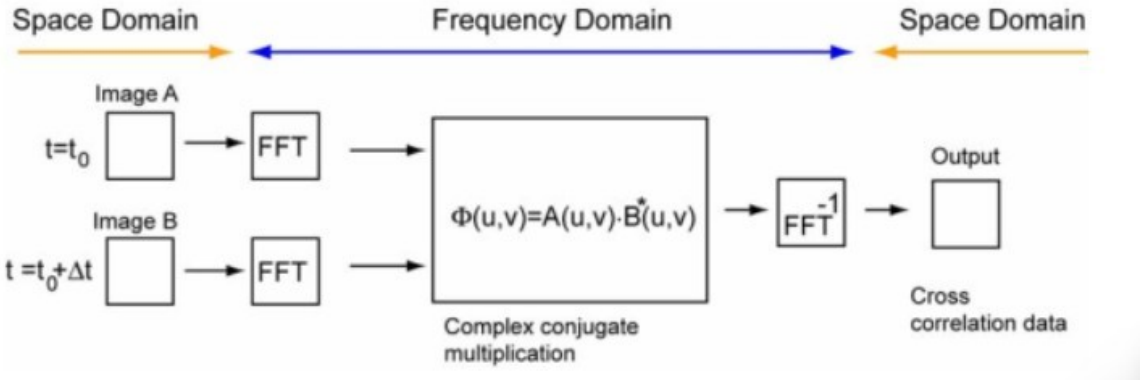

Figure 2.8: Cross-Correlation via FFT [4]

2.2.5 Validation and Interpolation

The presence of noise in images results in obervation of faulty vector fields. This problem is mitigated by the use of velocity based validation. Velocity thresholds are obtained by comparing images with lower and upper thresholds[3].

$$t_{lower} = \overline{u} - n * \sigma_u$$

$$t_{lower} = \overline{u} - n * \sigma_u$$

where $\overline{u}$ is mean velocity, σ_u is standard deviation of velocity and n is strictness of filter being used. This method helps remove outliers to make fields more uniform[3].
For empty spaces present as result of uneven intensity or uneven particle distribution, processing shows low velocity fields or no velocity fields; such errors are removed by Interpolation of missing data. Boundary Value Interpolation, such as one used by PIVLab, helps generate fairly smooth results. This method is advantageous when there are large regions of missing data as the use of boundary value velocity values for interpolation prevents overshooting[3].

2.3 Papers Reviewed

Perissonotto et al. [2] investigates the flow behavior in a centrifugal pump handling single-phase water flows. Using Particle Image Velocimetry (PIV) under varying conditions, the research reveals that flow uniformity decreases and turbulence increases as the pump operates away from its optimal efficiency point. These findings contribute to validating simulations, proposing models, and enhancing impeller designs.

Perissonotto et al. [8] claims that flow visualization has been crucial for the development of fluid mechanics. Recent advancements in cameras, lasers, and other technologies have enhanced the accuracy and reliability of techniques like High-Speed Imaging (HSI) and Particle Image Velocimetry (PIV). These techniques are now essential for studying centrifugal pumps. In this paper, Perissonotto et al. [8] review existing research on flow visualization in centrifugal pumps, comparing methods, examining their benefits and limitations, and suggesting future research to address current knowledge gaps.

The paper by Perissonotto et al. [5] presents an experimental study on flow dynamics within a centrifugal pump impeller. Utilizing a transparent pump prototype and time-resolved particle image velocimetry (TR-PIV), velocity fields were obtained under various operational conditions. Results show that flow behavior varies with impeller speed and water flow rate, affecting pump performance. These findings can aid in validating numerical simulations and proposing improvements in impeller design.

The study by Devkota et al. [6] uses Particle Image Velocimetry (PIV) to analyze flow behavior around a circular cylinder and a wing, with and without vortex generators (VGs). The research characterizes the PIV setup using the Strouhal number and analyze flow characteristics. Experimental data was processed using PIVLab and MATLAB.

Ciocanea et al. [10] claims use of multiple computer algorithms can be used to reverse engineer existing centrifugal pump impellers to maximize hydraulic efficiency. Simulation is used to obtain geometric configuration that gives best hydraulic efficiency.

Stepanoff's book "Centrifugal and Axial Flow Pumps: Theory, Design, and Application"[1] is a key reference for designing impellers and volute casings. The book offers practical insights into fluid

flow, velocity triangles, and energy conversion, providing essential design guidelines for vane angles, impeller dimensions, and casing geometry. Its empirical formulas and design charts help reduce hydraulic losses and improve pump efficiency. Stepanoff also addresses the design of pumps for handling abrasive, corrosive, and high-temperature fluids, offering strategies to prevent cavitation and ensure smooth operation. This reference supports a systematic approach to designing efficient and reliable pump components.

Dhungana et al. [11] details the design and fabrication of a Particle Image Velocimetry (PIV) setup to study low Reynolds number flow over a flat plate. Using a class 3B laser, high-speed camera, and smartphone camera, the setup captures flow data, which is analyzed with PIVlab in MATLAB. The study identifies flow features like laminar separation bubbles and vortex shedding, compares experimental results with numerical simulations, and highlights potential sources of errors in the setup and image processing.

CHAPTER 3
METHODOLOGY

The project is divided into two parts, i.e., design and fabrication of the Centrifugal pump test rig(Phase I) and conducting experiments and numerical simulation(Phase II). The process flowchart is given below:

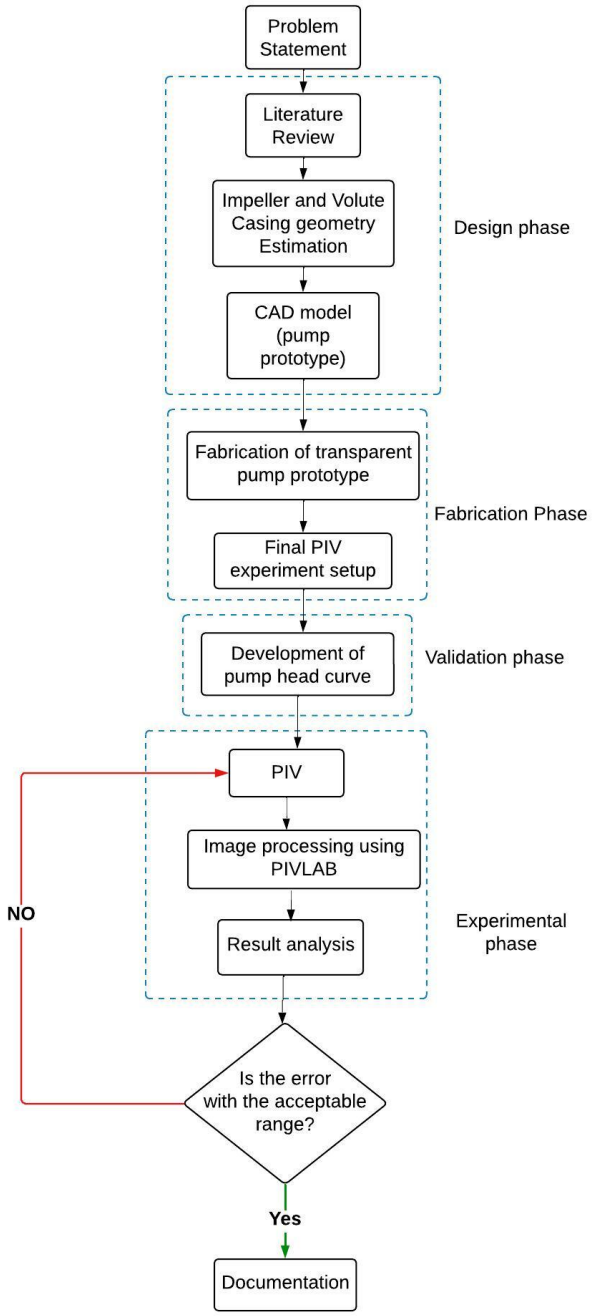

Figure 3.1: Methodology Flow Chart

Figure 3.2 shows the flow chart that explains the complete process involved in a flow field measurement

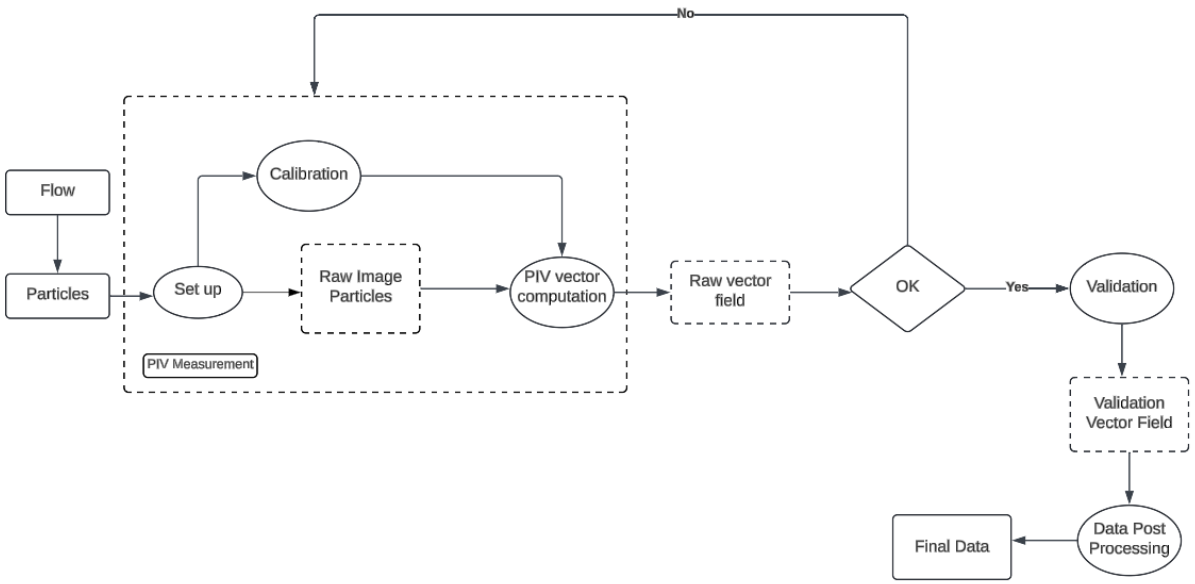

Figure 3.2: PIV Process Flowchart

using PIV.

3.1 Design Phase

3.1.1 Design Considerations

In order to keep the experimental setup very simple in our first attempt to apply the PIV technique in a rotating impeller, we have made some considerations. One design consideration was to maintain a closed-loop test rig, to avoid any irregularity while measuring the data of flow rates, head, and the PIV technique. It is done as we are interested in the flow phenomenon inside the impeller passages, rather than predicting the performance of a true pump stage[12]. With that main consideration kept in mind, the test rig for the experiments was designed to fulfill the following requirements:

- To enable us to study the flow phenomenon inside the impeller passages
- To have easy visual access inside the pump
- To gain a stable inlet velocity profile
- to vary the flow rate at different operating speeds. A main concern was to keep the setup as simple as possible while maintaining the true feature of the internal impler flow

3.1.2 Initial parameters Used

The design of the transparent centrifugal pump prototype for flow visualization was carefully developed to include key components such as the impeller (shroud and blades), volute casing, front plate, and rear plate. The parameters for the impeller and volute casing were determined based on the performance requirements and geometric constraints of the system, ensuring both accurate replication of the pump's operation and optimal performance for the Particle Image Velocimetry (PIV) experiment.

The design followed the key specifications of the ESP model P23, series 538, manufactured by Baker-Hughes, a widely used model in oil production. For this real-world ESP, when operating with water at 3500 rpm, the pump achieves a head of 17 meters and a flow rate of 15 m³/h per stage at its best efficiency point.[13] These specifications were used as a reference to ensure the transparent pump prototype would simulate realistic operating conditions.

Table 3.1: Pump Specifications at BEP

Parameter	**Value**
Manufacturer	Baker-Hughes
Model	ESP P23 series 538
Flow Type	Radial
Blades	7
Flow per stage [m^3/h]	15
Head [m]	17
Rotational Speed [rpm]	3500

The initial step in developing the transparent pump prototype involved fabricating acrylic glass models for the volute casing and impeller. Establishing precise design parameters for these components was essential to ensure the setup's functionality for accurate flow visualization and subsequent analysis.

3.1.3 Impeller

The impeller geometry of the pump prototype was derived from the electrical submersible pump (ESP), model P23, series 538 by Baker Hughes, as referenced in the work of Rodolfo et al. The CAD model was created using DS SolidWorks, and the design parameters of the impeller are presented in the table below.

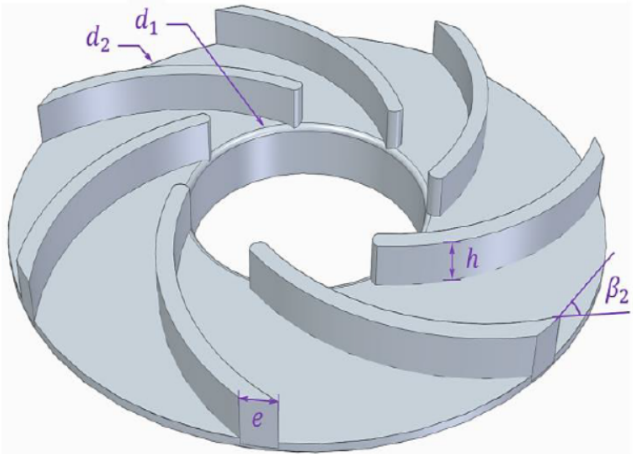

Figure 3.3: Impeller Parameter[5]

Table 3.2: Impeller known parameters

Parameter	**values**
Inlet diameter	d_1=44 mm
Outlet diameter	d_2=109 mm
Blade Angle at Outlet	β_2 = 46.8°
Blade thickness	e = 5.5 mm
Blade Height	h = 6.0 mm

3.1.4 Impeller blade

To simplify the manufacturing process, the impeller's shroud and blades were designed as separate components. This approach ensures easier fabrication, assembly, and precision in achieving the desired geometric accuracy.

3.1.5 Mid Section Volute

The design of the volute casing involves a series of calculations to ensure optimal performance and efficiency of the centrifugal pump.These are further described in the section below:

3.1.5.1 Specific Speed Calculations

The specific speed (n_s) is calculated to classify the pump type and guide the design. A.J. Stepanoff has provided the specific speed ranges for the centrifugal pump in the context of customary US units to be used (rpm, gpm, ft)[1]. The formula for specific speed is:

$$n_s = \frac{n \times \sqrt{Q}}{H^{3/4}}$$

Where:

- n is the rotational speed in rotations per minute (rpm),
- Q is the flow rate in gallons per minute (gpm),
- H is the head in feet (ft).[1]

The specific speed calculations for different operating conditions are summarized in Table 3.3.

Table 3.3: Specific Speed Calculations[2]

n [rpm]	Q [m^3/h]	Q [gpm]	H [m]	H [ft]	n_s
600	2.13	9.38	0.37	1.21	1588.8367
900	3.20	14.09	0.92	3.02	1475.2518
1200	4.26	18.75	1.71	5.61	1425.7011

The average of the above specific speed is 1497 RPM. Hence, taking 1500 RPM as the specific speed for the calculation of volute casing.

3.1.5.2 Determination of Volute Constants

The design elements of Volute casing which determine the hydraulic characteristics, namely volute angle(α_v), volute velocity constant(k_3),rotor diameter ($D2$) and volute diameter ($D3$) can be obtained from the fig-Volute Constants at specific speed 1500 RPM.

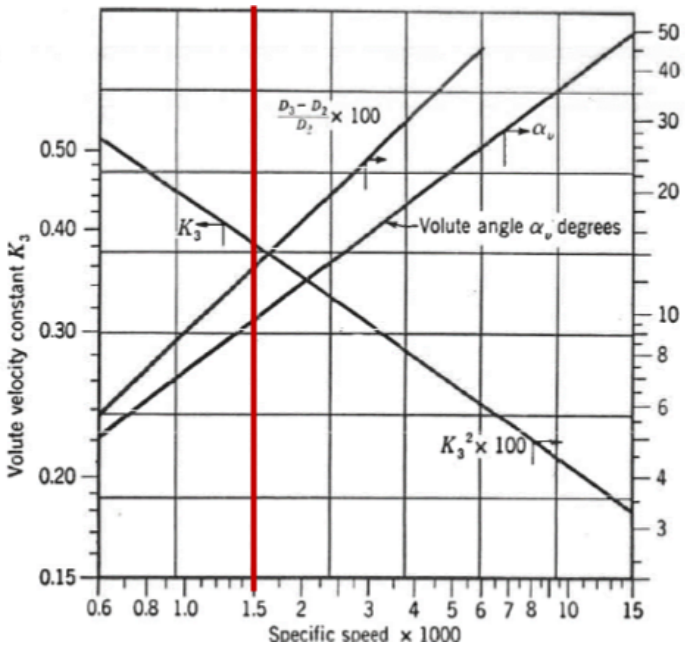

Figure 3.4: Volute Constants[1]

From Figure 3.4, The volute constants were obtained as:

- Volute Velocity constant(k_3) = 0.38
- Volute angle(α_v) = 10°
- $\frac{D_3-D_2}{D_2} = 0.13$

3.1.5.3 Average Fluid Velocity in the Volute

[1] The average fluid velocity c_3 in the volute is calculated using:

$$c3 = K_3 \times \sqrt{2gH}$$

Where k_3 is a constant, $g = 9.81 m/s^2$ and H is the head(m).

Table 3.4: Average Fluid Velocity in the Volute

n [rpm]	H [m]	c_3 [m/s]
600	0.37	1.02
900	0.92	1.61
1200	1.71	2.20

3.1.5.4 Calculation of Volute Geometry

][1] The volute geometry is defined based on the rotor diameter ($D2$) and the clearance factor ($K3$). The volute diameter ($D3$) is calculated as:

$$D3 = D2 \times (1 + \frac{D_3 - D_2}{D_2})$$

Where, $K_3 = 0.38$ and $D_2 = 109mm$
Hence, the volute diameter was obtained as 123.2mm.
The clearance between the rotor and volute is:

$$Clearance = D_3 - D_2$$

which was obtained as 14.2mm.
For Low specific speeds,the volute thickness ($b3$) is set to twice the rotor thickness ($b2$)[1]:

$$b3 = 2 \times b2$$

where, $b_2 = 6mm$
Hence, the rotor thickness was 12mm.
The maximum height of the volute ($h_{\max}$) is calculated as:

$$h_{\max} = \pi D3 \tan(\alpha_v)$$

The obtained maximum height was 68.23mm.
The area of the largest section of the volute is calculated as:

$$\text{Area} = b3 \times D3 \times \pi \times \sin(\alpha_v)$$

The obtained area of largest section of the volute was $806mm^2$.

3.1.6 Front Acrylic Plane

The front acrylic plane was designed to provide structural support and optical access for Particle Image Velocimetry (PIV) experiments in the transparent centrifugal pump assembly. The design was developed in SolidWorks, ensuring precise alignment with other components, with dimensions of 290 mm width, 210 mm height, and an extended section of 80 mm × 85 mm. A Ø49 mm hole was included for the inlet pipe, along with four Ø8.40 mm mounting holes for secure attachment. Acrylic sheets were chosen for their transparency, machinability, and chemical resistance, with material thickness optimized for strength and sealing. The design accounted for laser cutting and CNC machining, ensuring clean edges and accurate tolerances. Additionally, the plan incorporated waterproof adhesive sealant to prevent leakage, making the front acrylic plane an integral part of the experimental setup.

3.1.7 Rear Acrylic Plane

The rear acrylic plane, fabricated from black opaque acrylic, plays a crucial role in preventing light reflection and distortion in Particle Image Velocimetry (PIV) imaging, ensuring accurate flow visualization. Designed in SolidWorks, it has overall dimensions of 290 mm × 210 mm, with an 80 mm

extended section for structural integration. A Ø20 mm circular cutout is precisely made at the center to accommodate a nylon bushing with an inner diameter of 17 mm and an outer diameter of 20 mm, which securely holds the shaft. The shaft passes through this bushing and connects to the impeller inside the volute casing, ensuring smooth rotation and minimal vibration. Additionally, four Ø8.40 mm mounting holes are incorporated for secure attachment. The black acrylic material was specifically chosen to eliminate optical interference while maintaining structural integrity. Laser cutting and CNC machining were used to achieve high precision, ensuring proper alignment and a leak-proof assembly with waterproof adhesive sealant.

3.1.8 Pump Shaft

The pump shaft has been defined with specific dimensions to ensure a secure and functional connection between the impeller and the motor. The shaft has a total length of 87 mm, with the first 17 mm having a diameter of 17 mm. This section features two 3 mm holes, positioned 9 mm apart from center to center, to facilitate the attachment of the impeller using Allen bolts. The remaining 70 mm of the shaft has a diameter of 20 mm, with the 20 mm diameter section containing a 12 mm bore, 15 mm in length. This bore accommodates the 12 mm motor shaft, allowing for rigid coupling between the motor and the pump shaft. A set screw is used to ensure a secure connection and prevent any slippage between the motor and the pump shaft. The shaft is held in place by a nylon bushing, which is placed within a 20 mm diameter hole in the rear acrylic plane. The nylon bushing has an internal diameter of 17 mm, ensuring a snug fit for the 17 mm diameter section of the shaft. This arrangement provides additional support and stability for the shaft, minimizing any potential movement or vibrations during operation, while reducing friction and wear on both the shaft and the acrylic plane.

3.1.9 Pump Assembly

The pump assembly consists of several key components that are securely joined together to form a functional unit. These components include the front acrylic plane, midsection volute, rear acrylic plane, impeller shaft, nylon bushing, and oil seal. The assembly process involves the precise alignment and bonding of these parts to ensure proper functioning and leak-free operation.

The front acrylic plane and rear acrylic plane are laser-cut and CNC-machined to fit the volute and shaft components. The midsection volute, also laser-cut, is designed to house the impeller and direct the flow of fluid efficiently. The impeller shaft is inserted into the nylon bushing, which is placed within the 20 mm diameter hole in the rear acrylic plane. This bushing ensures that the shaft is securely held in place, reducing friction and wear.

To ensure a watertight seal, an oil seal is placed around the shaft in the appropriate location, preventing any fluid leakage from the assembly. All components are bonded together using UV glue, which provides a strong, durable adhesive to hold the parts in place. The UV glue ensures that the assembly is rigid and leak-proof, offering the required structural integrity for the pump to operate smoothly and efficiently.

3.2 CAD Model

The experimental setup was divided into 6 sub-assemblies as mentioned in the above sections. Each sub-assembly was designed separately, and the final assembly of all the components was carried out.

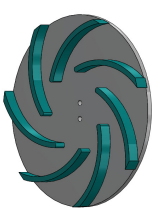

((a)) Impeller CAD model

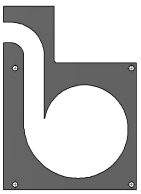

((b)) Volute CAD model

Figure 3.5: CAD models of pump components: (a) impeller and (b) volute

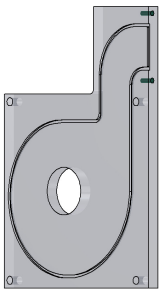

((a)) Front Plane CAD model

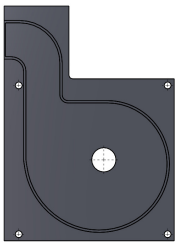

((b)) Rear Plane CAD model

Figure 3.6: Acrylic plane CAD models showing front and rear views

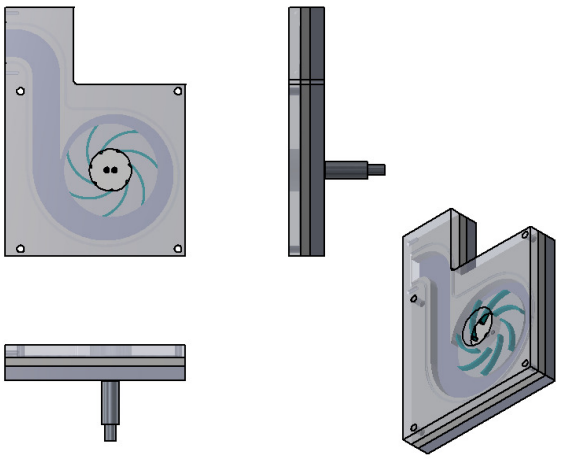

Figure 3.7: Pump Assembly

3.3 Fabrication Phase

The transparent impeller and volute casing were fabricated using acrylic sheets, selected for their excellent optical clarity, ease of machining, durability, and chemical resistance. These properties ensure minimal distortion and optimal transparency for Particle Image Velocimetry (PIV) experiments, allowing precise observation of fluid movement within the pump.

Figure 3.8: Fabricated Acrylic Parts(Before Assembling)

3.3.1 Impeller Fabrication

The impeller design consists of multiple blades and a shroud. The impeller blades were cut from acrylic sheets using a laser cutting machine, ensuring smooth edges and high dimensional accuracy. The grooves in the impeller shroud, where the blades are placed, were machined using a CNC machine for precise fit and alignment. Afterwards, the individual blades and shroud were bonded together using UV glue, which provides a strong, transparent, and durable joint without compromising optical clarity.

3.3.2 Volute Casing Fabrication

The volute casing, housing the impeller, was machined from acrylic sheets following the CAD model specifications. Laser cutting was employed for the outer edges of the volute casing, while CNC machining was used to create precise grooves in the front and rear acrylic planes. The front acrylic plane, volute casing, and rear acrylic plane (made from black opaque acrylic) were aligned and assembled using the laser-cut impeller and shaft, with UV glue securing the components. A waterproof adhesive sealant was applied at all joints to prevent leaks and ensure structural integrity.

3.3.3 Shaft Assembly

The shaft was connected to the rear plane using a nylon bushing. An oil seal was inserted between the shaft and rear plane to prevent any leakage.
This meticulous fabrication process ensures that the impeller and volute casing meet the required standards for optical clarity and functional performance in the PIV experiment.

3.3.4 Experimental Setup

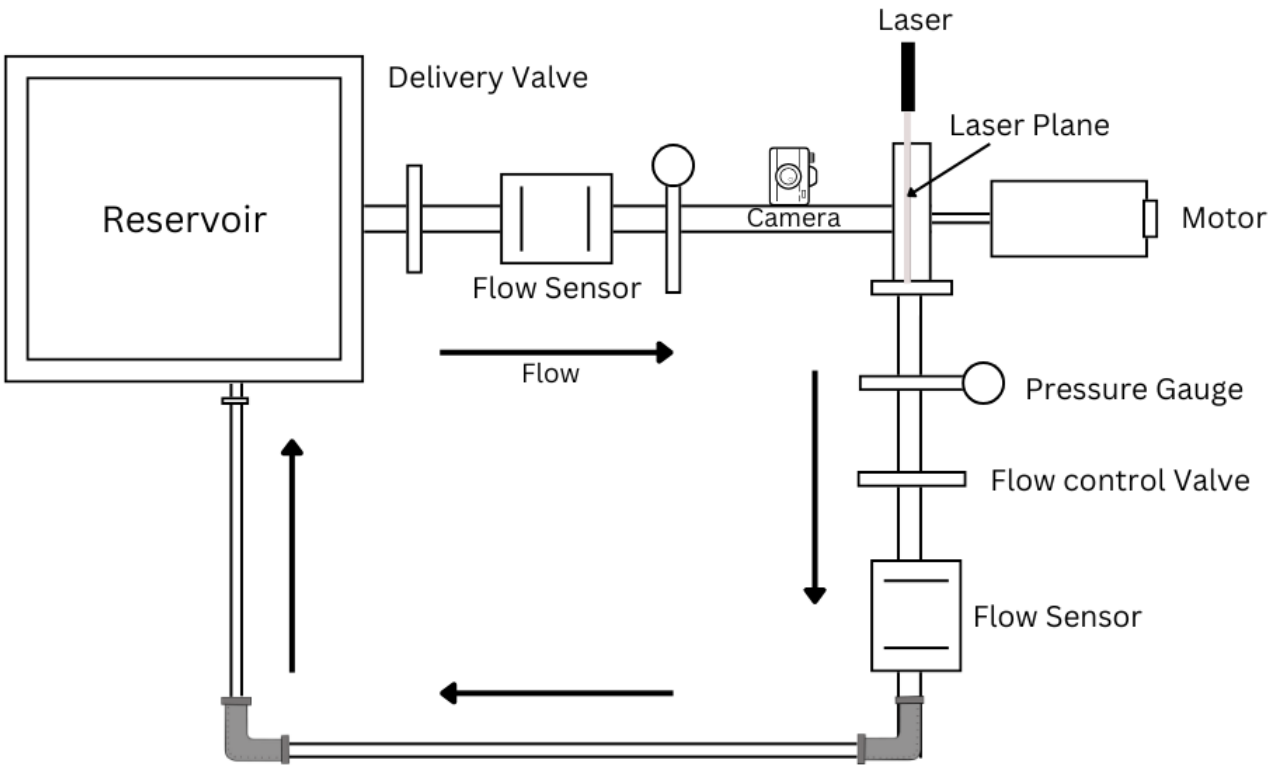

Figure 3.9: Schematic Diagram of Experimental PIV Setup

The fabricated transparent centrifugal water pump was coupled with an electric motor (0.18 kW/0.25 HP) using a 20mm diameter shaft. This coupling ensures that the motor drives the impeller efficiently for fluid flow. The entire setup was assembled, including a reservoir containing water seeded with particles, using appropriate pipes and fittings.
The pump's outlet was also connected to the same reservoir, as shown in the schematic diagram below. The motor primes the impeller, and the centrifugal pump draws in water, which will be analyzed using Particle Image Velocimetry (PIV). The PIV measurement instruments, including the camera and laser, were incorporated into the experimental setup to capture the flow dynamics. These instruments will allow for precise measurement and visualization of the fluid flow, aiding in the analysis of the pump's performance.
This setup ensures proper fluid circulation and provides the necessary components for conducting accurate PIV experiments.

3.4 Simulation Phase

The simulation of the centrifugal pump impeller began in Vista CPD, where key parameters such as head(17m), flow rate($15m^3/hr/stage$), number of blades(7), exit blade angle(46.8^0), and rotational

speed (1100*RPM*) were based on the original Baker Hughes 538 series pump impeller. Using these inputs, the necessary impeller and volute calculations and profiles were generated. The data from Vista CPD was then imported into BladeGen, where the blade shapes were refined by defining the trailing and leading edges as elliptical profiles. This BladeGen model was subsequently transferred to TurboGrid for high-quality meshing. After the mesh generation, the setup continued in CFX-Pre, where the mesh and previous design inputs were brought together, and the boundary conditions — specifically the outlet pressure and inlet mass flow rate — were defined. Using the SST turbulence model, the simulation was solved over 1000 iterations, leading to a fully converged and reliable result.

Table 3.5: Pump Performance Data

Parameter	**Value**	**Units**
Rotation Speed	115.1920	rad/s
Reference Diameter	0.1060	m
Volume Flow Rate	0.0001	m^3/s
Head (LE-TE)	4.0568	m
Head (IN-OUT)	3.3031	m
Flow Coefficient	0.0009	–
Head Coefficient (IN-OUT)	0.2173	–
Shaft Power	7.0759	W
Power Coefficient	0.0003	–
Total Efficiency (IN-OUT)	54.2063	%
Static Efficiency (IN-OUT)	32.0001	%

The table 3.5 outlines the essential performance metrics for a centrifugal pump functioning at a rotational speed of 115.19 rad/s, featuring an impeller reference diameter of 0.106 m and a flow rate of 0.0001 m³/s. It indicates that the pump produces a head of 4.06 m from the leading edge to the trailing edge of the impeller, and a net head of 3.30 m from the inlet to the outlet, demonstrating the energy transferred to the fluid. The flow and head coefficients, which are both dimensionless, facilitate the comparison of pump performance across various designs and operational scenarios. The shaft power demand is recorded at 7.08 W, and the power coefficient supplies a normalized assessment of this energy input. Importantly, the total efficiency, calculated on the basis of total head, stands at 54.21%, while the static efficiency, which is based solely on pressure increase, is measured at 32%, indicating the pump's effectiveness in transforming input mechanical energy into beneficial hydraulic energy.

This figure 3.10 shows the distribution of total pressure (Pt) at the midpoint span of a centrifugal pump impeller. The image is a cross-sectional representation located halfway between the hub and the shroud, illustrating how pressure varies as fluid flows through the rotating blades of the impeller. The color scale on the left displays total pressure values, ranging from negative values (represented by dark blue) to 40,000 Pa (indicated by red). As the fluid enters from the left (the low-pressure side), it travels through the gaps between the impeller blades (represented by the white curved shapes), and its total pressure progressively increases, evidenced by the transition from blue to green, yellow, and finally orange and red toward the outer edge. This increasing pressure illustrates how the impeller adds energy to the fluid, enhancing its total pressure as it advances toward the pump outlet, which is the primary function of a centrifugal pump.

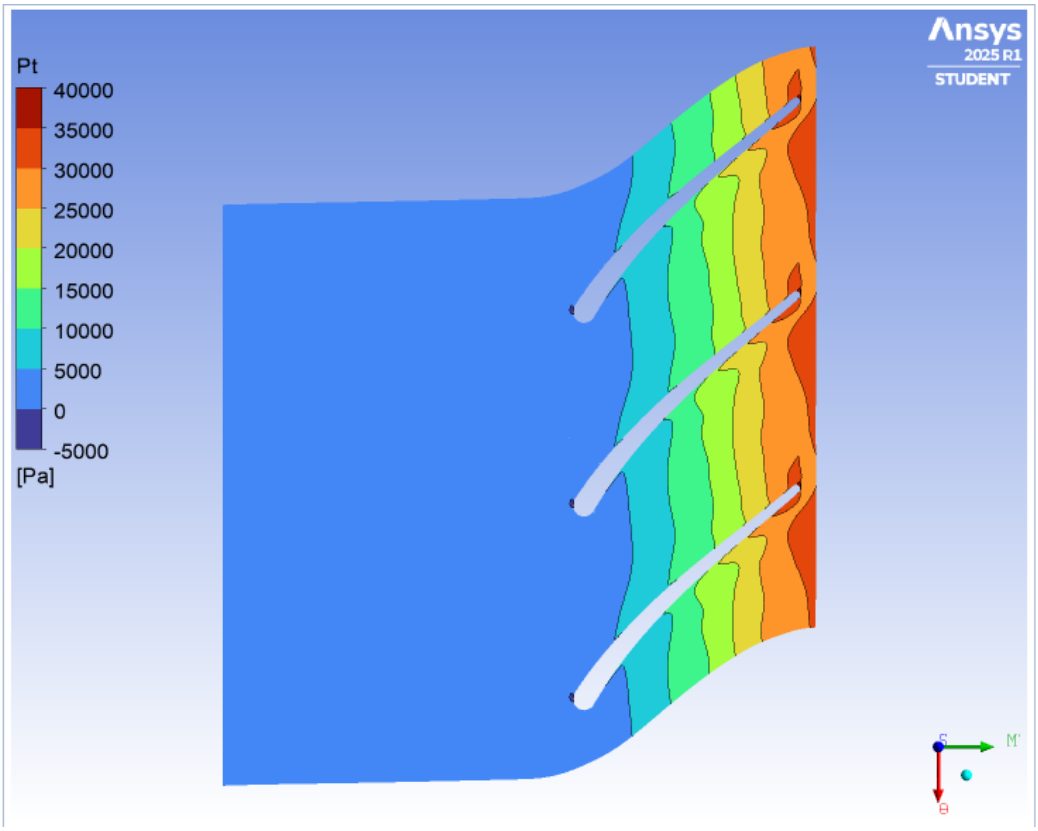

Figure 3.10: Contour of Total Pressure (pt) at 50% span

The figure 3.11 shows the static pressure (Ps) contour plot at the halfway point of a centrifugal pump impeller, highlighting the key pressure transformation mechanism within the pump. The image depicts three curved impeller blades (colored in white/gray) that impart energy to the fluid as they spin, with a distinct pressure progression from the inlet area (represented in dark blue, indicating a negative pressure around -2000 Pa) to the outlet edge (shown in red, reaching about 20,000 Pa). The fluid enters from the left side, where the pressure is lowest, especially near the leading edges of the blades, and as it moves through the curved channels between the blades, it undergoes a gradual increase in pressure (transitioning through light blue, green, yellow, and orange) due to the centrifugal force and energy transfer from the spinning impeller. This visualization of the pressure gradient at the mid-span cross-section effectively illustrates how the mechanical energy from the spinning impeller is converted into fluid pressure energy, which is the essential function of a centrifugal pump.

This Figure 3.12 depicts a velocity contour and vector diagram illustrating the flow field at the 20% span of a centrifugal pump impeller. The background hues signify fluid velocity magnitude, with blue representing slower speeds and transitioning from green to red for higher speeds, as indicated on the color bar to the left (ranging from 0 to 3.8 m/s). The black arrows depict both the direction and relative strength of the fluid velocity at various locations. On the left side of the illustration, prior to the impeller blades, the flow is comparatively uniform and steadily directed towards the impeller. As the fluid approaches the impeller area on the right, the velocity distribution grows more intricate: blue areas indicate low velocity near the blade surfaces, while green/yellow highlights higher velocities in the gaps between the blades. The swirling patterns and variations in arrow direction around the blades

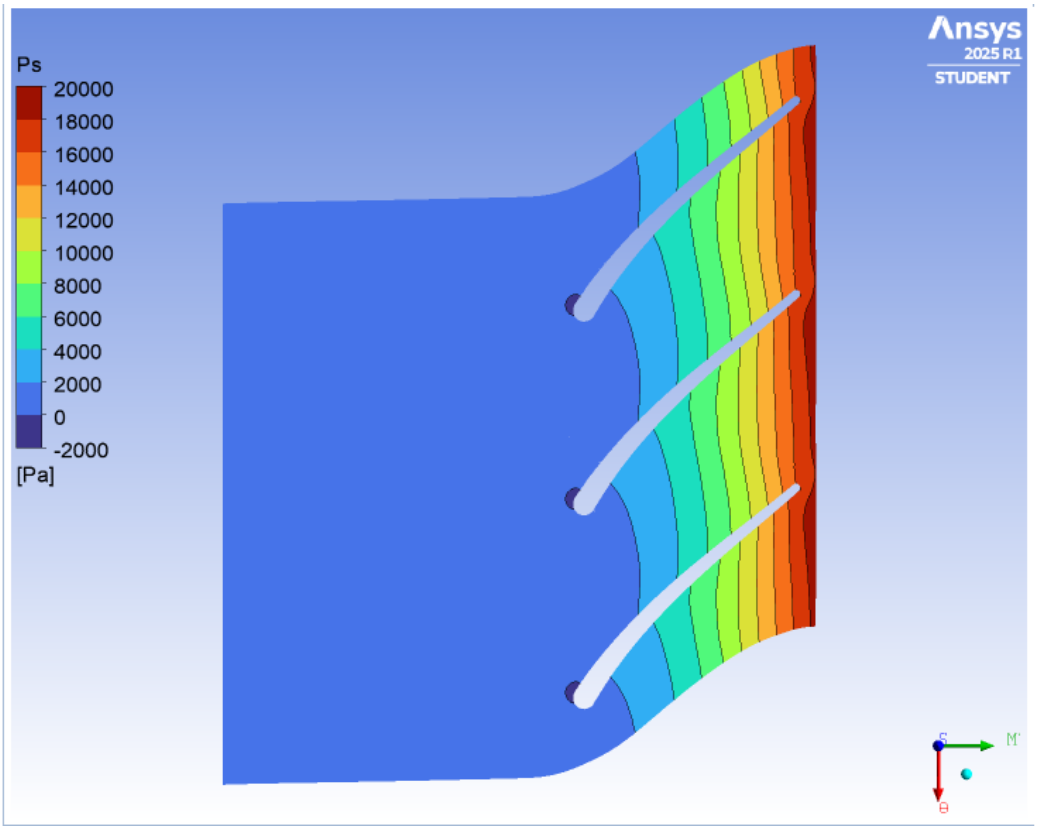

Figure 3.11: Contour of Static Pressure (ps) at 50% span

demonstrate significant flow rotation and recirculation, commonly seen in the impeller region as the rotating blades add energy to the fluid and redirect its flow outward. This visualization assists engineers in analyzing how effectively the impeller is enhancing the fluid's velocity and determining if any unwanted flow patterns, such as recirculation or stagnation, are occurring.

This figure 3.13 displays a velocity contour and vector diagram depicting the fluid flow within a centrifugal pump impeller at a 50% span. The background hue indicates the fluid velocity magnitude, with blue corresponding to lower speeds and green to yellow representing higher speeds, as denoted by the color scale on the left (ranging from 0 to 3 m/s). The black arrows indicate both the direction and relative strength of the fluid velocity at various points. On the left side, prior to entering the impeller blades, the flow appears fairly uniform and directed toward the impeller. As the fluid progresses through the curved channels between the spinning impeller blades, the velocity distribution becomes increasingly intricate: the velocity rises within the passages (green/yellow), while areas adjacent to the blade surfaces display lower velocities (blue). The swirling patterns and variations in arrow direction near the blades illustrate how the rotating impeller reorients and accelerates the fluid, showcasing the energy transfer mechanism that is essential to the functioning of a centrifugal pump. This visualization facilitates the identification of how effectively the impeller moves the fluid and emphasizes any zones where flow separation or recirculation might take place.

The figure 3.14 is a velocity contour and vector diagram depicting the fluid flow within a centrifugal pump impeller at 80% span. The background hue indicates the fluid's velocity magnitude, with blue signifying lower speeds and transitioning from green to red for higher speeds, as detailed by the color

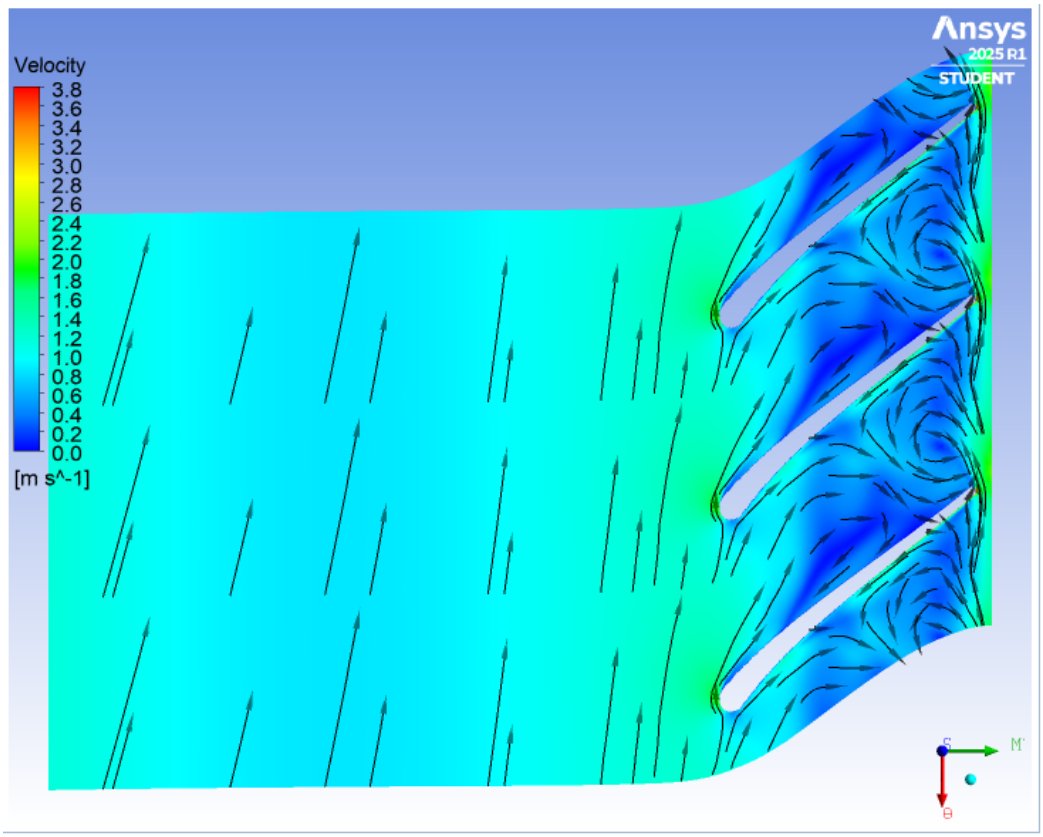

Figure 3.12: Velocity Vector at 20% span

bar on the left (spanning from 0 to 2.4 m/s). The black arrows represent both the direction and relative magnitude of the fluid velocity. Before the fluid enters the impeller blades on the left, it exhibits a fairly uniform flow directed toward the impeller. As the fluid flows through the curved channels between the rotating impeller blades, its velocity increases (evidenced by the shift from blue to green and orange near the blade tips), resulting in more intricate flow patterns, including swirling and recirculation near the blade surfaces. This visualization effectively demonstrates how the impeller accelerates and redirects the fluid, a critical aspect of the pump's functionality, and it also emphasizes areas where flow separation or recirculation might occur, potentially impacting pump efficiency.

The figure 3.15 shows the velocity streamlines around the trailing edge of the blades. The colors represent the flow velocity, where blue indicates low-speed regions and red indicates high-speed regions. As the flow moves past the blades, it forms a wake characterized by lower velocities and chaotic, swirling patterns, especially near the trailing edge. These swirling motions are small vortices created due to flow separation, where the fluid cannot stay attached to the blade surface. The wake region, seen clearly with blue and green colors, highlights the energy loss that naturally occurs behind the blades. Additionally, near the blade tips, the streamlines become more distorted, indicating the formation of tip vortices, which further contribute to aerodynamic losses. Overall, the plot captures how the flow behaves after leaving the blade, with slower, disturbed flow regions forming behind the trailing edge.

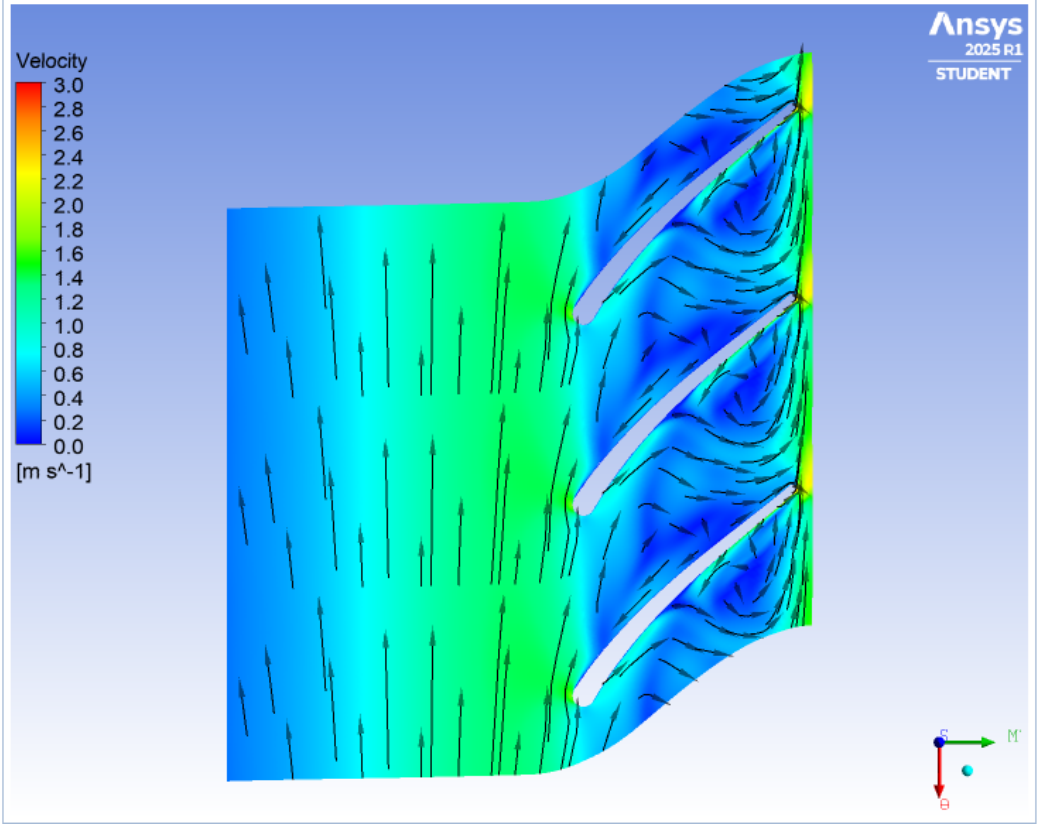

Figure 3.13: Velocity Vector at 50% span

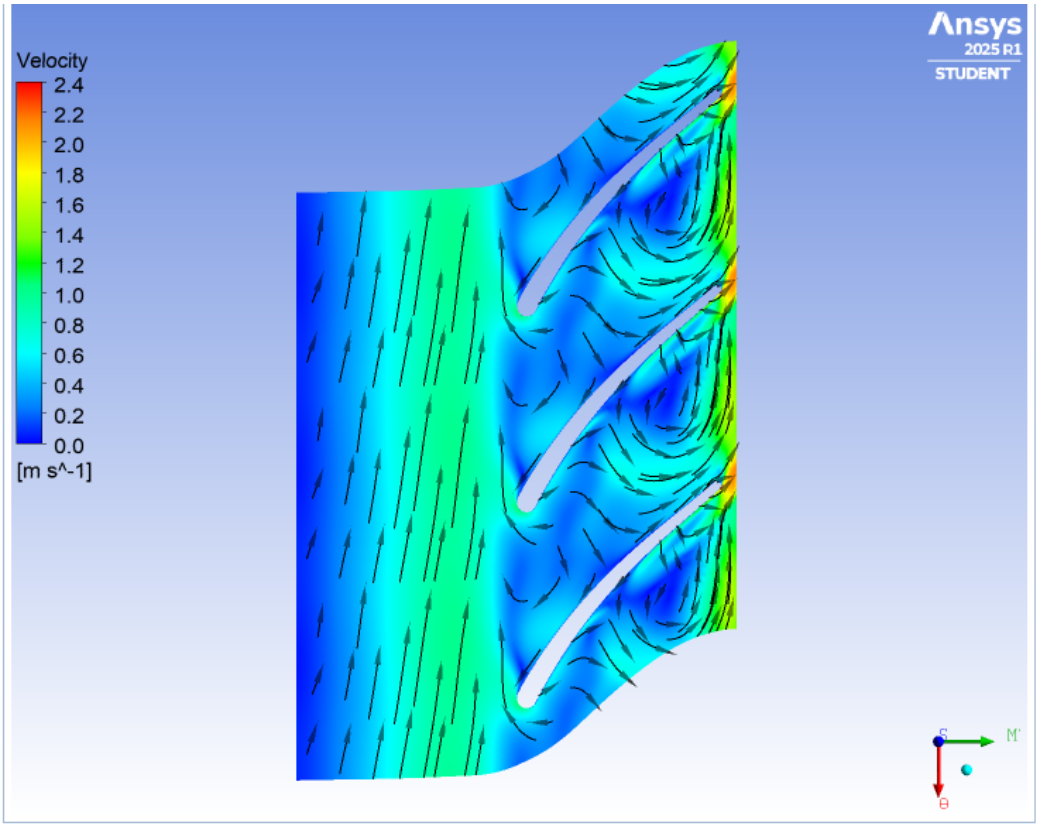

Figure 3.14: Velocity Vector at 80% span

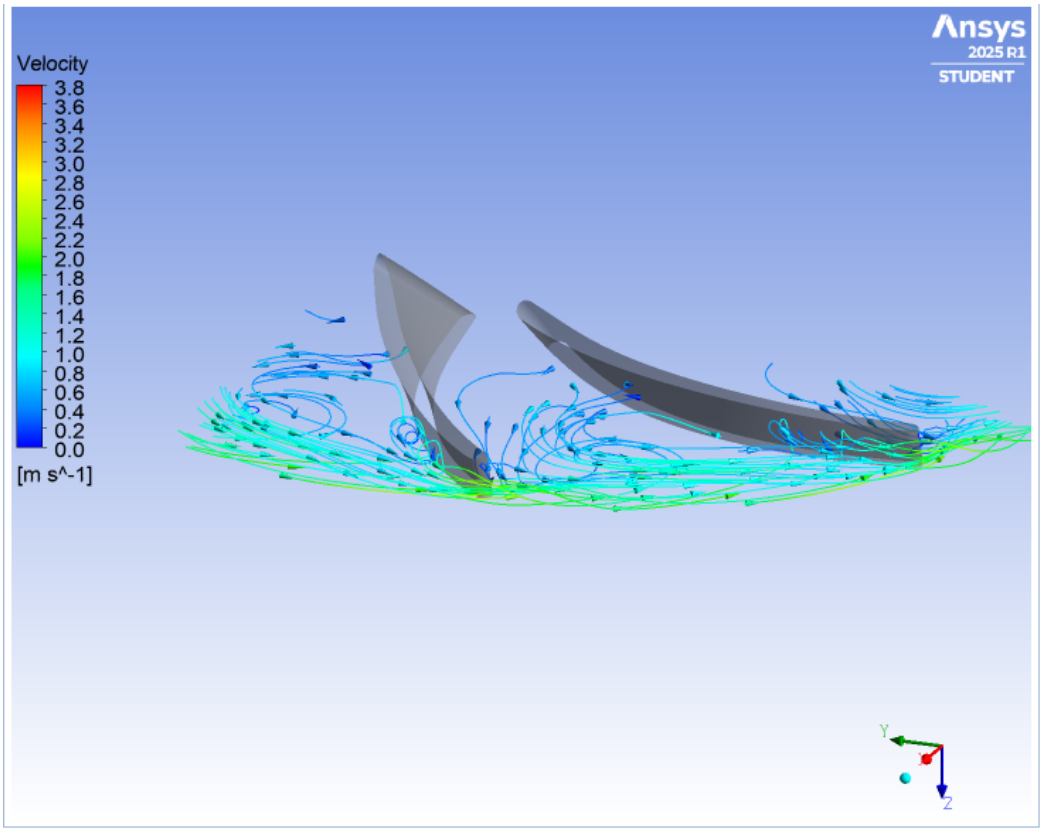

Figure 3.15: Velocity streamlines at Blade Trailing Edge

3.5 Validation phase

3.5.1 Theoretical Pump Head Curve

3.5.1.1 Defining Pump Geometry and Parameters

The impeller outlet diameter (d_2) , blade angle at outlet (β_2), blade height (b_2), and blade thickness (t) were determined based on the pump design specifications. Additional parameters such as the number of blades (Z), gravitational acceleration (g), and water density (ρ) were also defined.

3.5.1.2 Establishing Operating Conditions

The analysis was conducted at two different rotational speeds:

$$N1 = 1000RPM$$

with an input power of

$$P_{input1} = 7.69439W$$

$$N2 = 1100RPM$$

with an input power of

$$P_{input2} = 10.241238W$$

The maximum flow rates were determined based on experimental observations.

3.5.1.3 Theoretical Head and Efficiency Calculation

The theoretical head (H) was computed using Euler's turbomachinery equation:

$$H = \frac{u_2 \cdot v_{u2}}{g}$$

where: $u2 = \frac{\pi d_2 N}{60}$ is the blade tip speed.

$v_{u2} = u_2 - \frac{v_{f2}}{\tan(\beta_2)}$ is the tangential velocity component of water.

$vm2$ is the meridional velocity, calculated from the flow rate and impeller outlet area.

The hydraulic efficiency (η) was determined using:

$$\eta = \frac{\rho g Q H}{P_{input}} \times 100$$

3.5.2 Head-capacity Relations

The theoretical head (H) was computed using Euler's turbomachinery equation:

$$H = \frac{u_2 \cdot v_{u2}}{g}$$

$$H_e = \frac{V_{W2} u_2}{g} = \frac{u_2}{g}[u_2 - V_{f2} \cot\beta]$$

$$H_e = \frac{u_2}{g}\left[u_2 - \frac{Q}{A_2} \cot\beta\right]$$

For a particular pump running at a constant speed, the blade velocity $u2$, blade exit angle β, and area A_2 are fixed. The above equation can also be expressed as,

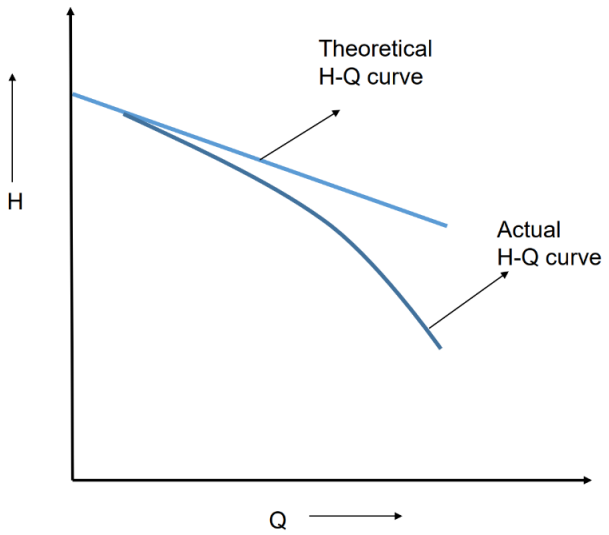

Figure 3.16: Difference between actual and theoretical curve

$$H_e = K_1 - K_2 * Q$$

Which is a straight line whose slope is fixed by angle β.
Where, K_1 and K_2 are constants which are determined by shut-off head conditions and maximum flow rate, and Q is the Flow rate. The expression for K_1 and K_2 are:

$$K_1 = \frac{u_2^2}{g}$$

$$K_2 = \frac{u_2 * cot\beta}{A_2 * g}$$

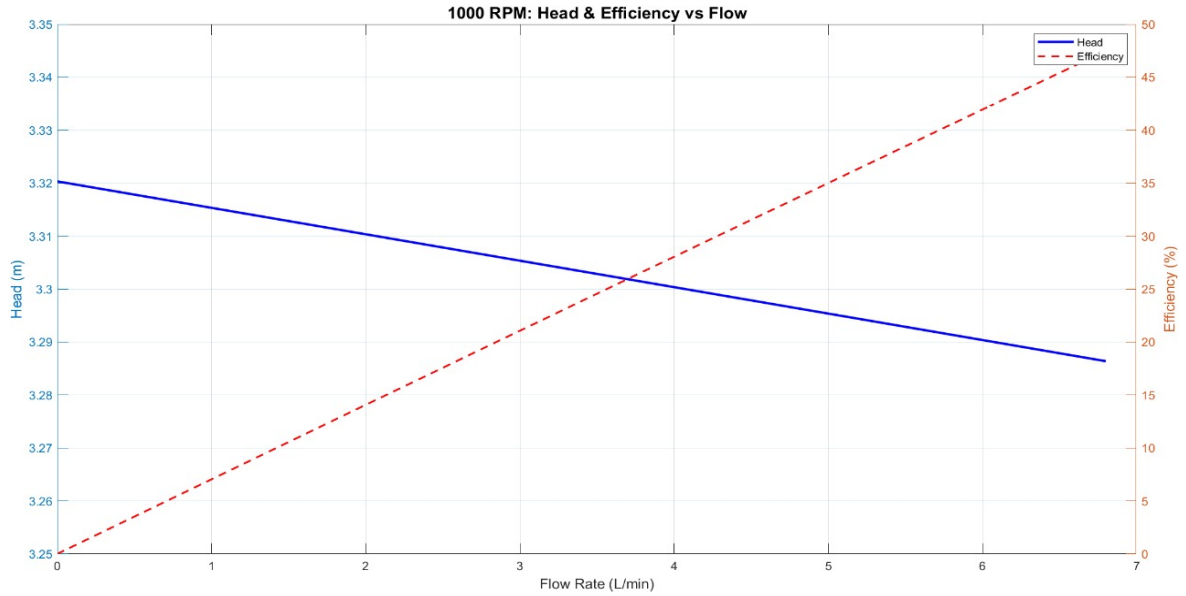

((a)) At 1000 RPM

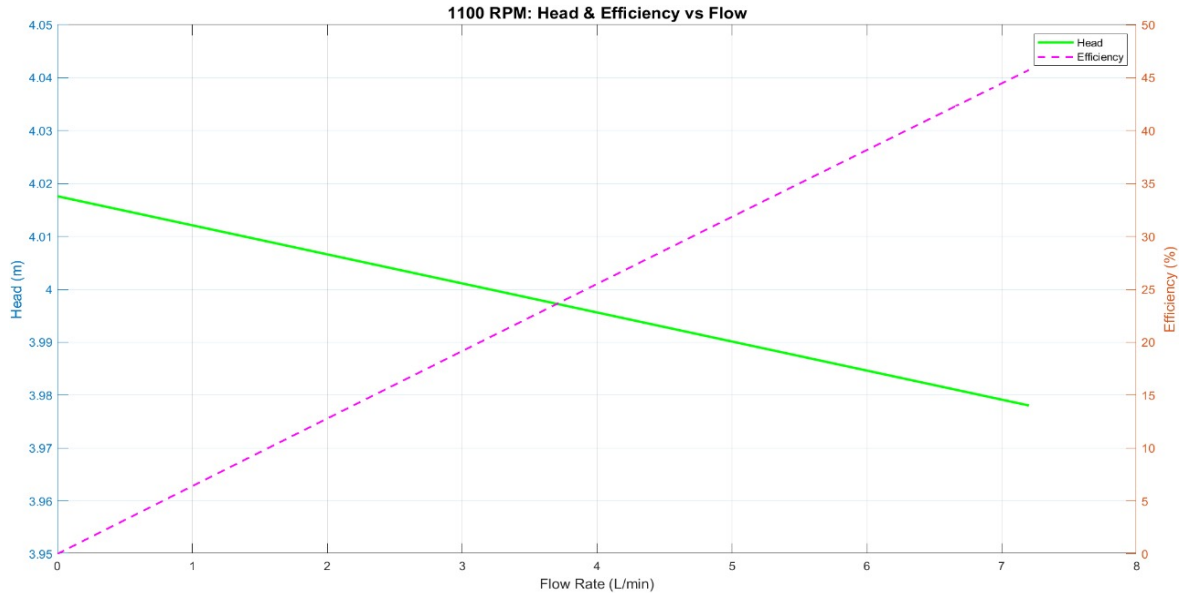

((b)) At 1100 RPM

Figure 3.17: Theoretical Pump Head Curve

3.5.2.1 Curve Generation and Visualization

To smooth the discrete data points and generate continuous curves, a Piecewise Cubic Hermite Interpolating Polynomial (PCHIP) method was applied. This method ensures that the curves are smooth and exhibit continuous first derivatives, which is crucial for accurate analysis of pump performance. The theoretical head and efficiency values were calculated across a range of flow rates. Smooth head-efficiency curves were plotted for both speeds using MATLAB.
The figure 3.17(a) illustrates the theoretical performance of the pump at 1000 RPM, displaying both head and efficiency as a function of flow rate. The blue line indicates the head, which remains nearly constant at approximately 3.3 meters, with a very slight decline as the flow rate rises. This pattern is characteristic of theoretical models where friction losses are minimized and ideal conditions are considered. Conversely, the red dashed line shows the efficiency, which linearly increases with flow rate, beginning at around 0% for zero flow and approaching nearly 45% at the maximum flow rate of approximately 6.5 liters per minute. Unlike experimental curves, where efficiency typically peaks and subsequently decreases, this efficiency continually ascends, indicating that under ideal conditions, the pump would become more efficient at higher flow rates without the decline observed in actual performance. This graph emphasizes the idealized expectation of the pump: a consistent head and a progressive enhancement in efficiency as flow rate increases.

The figure 3.17(b) illustrates the theoretical operation of the pump at 1100 RPM, charting head and efficiency in relation to flow rate. The green line depicts the head, remaining nearly constant at around 4 meters, with a very slight decline as the flow rate rises. This pattern is typical in theoretical models where factors like friction are reduced, and ideal situations are presumed. Conversely, the magenta dashed line signifies the efficiency, which increases linearly with the flow rate, beginning at approximately 0% with no flow and approaching nearly 45% at the maximum flow rate of about 7 liters per minute. Unlike the experimental curves, where efficiency reaches a peak and then decreases, here the efficiency steadily increases, indicating that under ideal conditions, the pump would become more efficient at greater flow rates without the decline observed in real-life performance. This graph emphasizes the idealized expectation for the pump: a consistent head and a continuous rise in efficiency as the flow rate advances.

3.5.2.2 Numerical Output

The theoretical head and efficiency values were tabulated. For 1000 RPM, the values are tabulated in Table 3.6. From the simulation, we determined the overall efficiency to be 54.21%, which closely matches the theoretical efficiency calculated here(47.49%),confirming the accuracy of the simulation results.

3.5.3 Actual Pump Head Curve

To analyze the performance of the centrifugal pump, the actual head curve was generated using experimental data collected at two different rotational speeds, $1000RPM$ and $1100RPM$. The following steps were performed:

3.5.3.1 Data Collection

The flow rate (Q) and head (H) values were measured and recorded for both $1000RPM$ and $1100RPM$ speeds.

Table 3.6: Theoretical Pump performance characteristics at different RPM

1000 RPM			1100 RPM		
Flow (LPM)	Head (m)	Eff. (%)	Flow (LPM)	Head (m)	Eff. (%)
0	3.3203	0	0	4.0176	0
0.75	3.3166	5.298	0.75	4.0134	4.8683
1.5	3.3147	7.9425	1.5	4.0112	7.4144
2.25	3.3092	15.619	2.25	4.0053	14.575
3.0	3.3046	22.314	3.0	4.0003	20.333
3.75	3.3011	27.085	3.75	3.9963	24.7
4.5	3.2976	31.846	4.5	3.9922	29.516
5.25	3.2939	37.071	5.25	3.988	34.323
6.0	3.2903	42.048	6.0	3.9844	38.663
6.8	3.2864	47.486	7.2	3.9781	45.727

The input of power (P) to the pump was also measured for each speed, ensuring accurate data for the calculation of efficiency.

3.5.3.2 Efficiency Calculation

The efficiency (η) of the pump was calculated using the hydraulic power equation, which expresses the relationship between the flow rate, head, and input power:

$$\eta = \frac{\rho g H Q}{P_{\text{input}}} \times 100$$

In this equation, P_{input} is the power input, Q is the flow rate, H is the head, ρ is the density of water $(1000\,\text{kg/m}^3)$, and g is the acceleration due to gravity $(9.81\,\text{m/s}^2)$. This formula was used to calculate the efficiency at various points for each speed.

3.5.3.3 Data Interpolation and Plotting

To smooth the discrete data points and generate continuous curves, a Piecewise Cubic Hermite Interpolating Polynomial (PCHIP) method was applied. This method ensures that the curves are smooth and exhibit continuous first derivatives, which is crucial for accurate analysis of pump performance.

The head and efficiency curves were then plotted against the flow rate (Q) for both speeds ($1000RPM$ and $1100RPM$) using MATLAB. This allowed visualization of the performance trends at different operating points.

At 1000 RPM, the pump exhibits typical characteristics where the head and efficiency vary with flow rate. When the flow rate is minimal, the pump achieves its maximum head of approximately 1.3 meters, indicating its capability to lift water significantly when flow is negligible. However, as the flow rate rises, the head steadily declines, reaching about 0.5 meters at the peak measured flow of around 6.5–7 liters per minute. This decline is expected, as pumping more water generally diminishes the lift capacity. Simultaneously, the pump's efficiency, which starts off quite low (nearly 0% at very low flow rates), progressively increases with higher flow rates, peaking at roughly 7.5% between 4.5 to 5

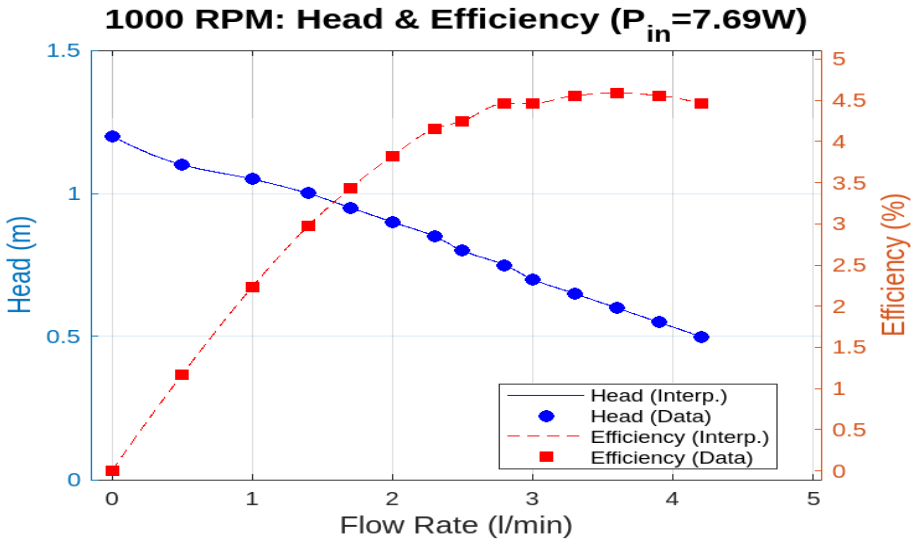

((a)) At 1000 RPM

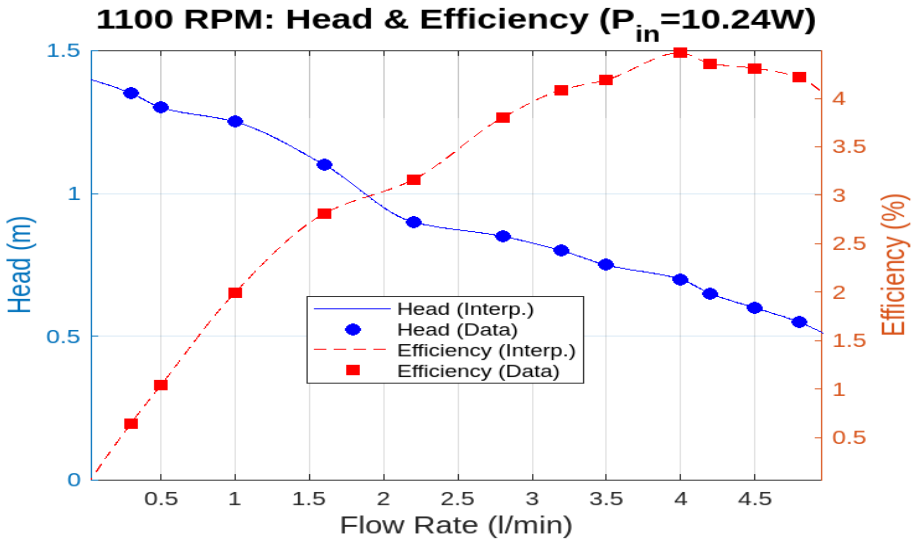

((b)) At 1100 RPM

Figure 3.18: Actual Pump Head Curve

liters per minute. After this peak, efficiency experiences a slight decrease at greater flow rates. This pattern indicates that the pump operates at its most efficient levels during moderate flow rates, rather than at the extremes of very low or very high flows. In summary, the curve indicates that for optimal efficiency, the pump at 1000 RPM performs best around 4.5–5 l/min, despite its overall efficiency remaining relatively low (below 8%), which is typical for small, low-power pumps with an input power of just 7.69 Watts.

At 1100 RPM, the pump exhibits behavior similar to that at 1000 RPM, but with a minor enhancement in performance. The head starts at a higher initial value of around 1.4 meters when the flow rate is very minimal, and then it steadily declines as the flow rate increases, reaching approximately 0.5 meters at the peak flow rate of about 7.2 liters per minute. This indicates that the pump can elevate water slightly higher at 1100 RPM compared to when it operates at 1000 RPM. The efficiency demonstrates a similar trend: it is quite low at nearly zero flow but progressively rises with the flow rate, achieving a maximum efficiency of roughly 7% around 6 liters per minute, followed by a slight

decrease at higher flow rates. In comparison to 1000 RPM, the ranges for flow rate and peak efficiency shift somewhat higher, illustrating that the pump performs more effectively at increased speeds. The input power also ramps up to 10.24 Watts, which is anticipated since more energy is required to operate the pump at a faster pace. Overall, operating the pump at 1100 RPM leads to a higher flow rate and marginally improved efficiency, though the maximum efficiency remains relatively low, as is typical for small experimental pumps.

3.5.3.4 Numerical Output and Analysis

The head and efficiency values were systematically tabulated for each data point, providing a clear record of the pump's performance at various flow rates.
The maximum efficiency point for each speed was identified by analyzing the efficiency curve. This allowed comparison of performance at the two different speeds and provided insights into the optimal operating conditions for the pump.

Table 3.7: Pump performance at different RPM

	1000 RPM ($P_{\text{input}} = 7.69$ **W**)			**1100 RPM** ($P_{\text{input}} = 10.24$ **W**)		
S.N.	**Flow (L/min)**	**Head (m)**	**Eff. (%)**	**Flow (L/min)**	**Head (m)**	**Eff. (%)**
1	0	1.2	0	0	1.4	0
2	0.5	1.2	1.28	0.3	1.4	0.67
3	1.5	0.95	3.03	0.53	1.3	1.10
4	2.27	0.9	4.34	1.6	1.2	3.07
5	3	0.85	5.42	2.8	1	4.47
6	3.73	0.85	6.74	3.6	0.9	5.17
7	4	0.8	6.80	4.8	0.8	6.13
8	4.27	0.75	6.81	5.33	0.75	6.38
9	5.07	0.7	7.54	6	0.7	6.71
10	5.6	0.65	7.73	6.8	0.65	7.06
11	6	0.6	7.65	7	0.6	6.71
12	6.8	0.5	7.22	7.2	0.5	5.75

Maximum Efficiency at 1000 RPM: 7.86% at 4.93 L/min, Head = 0.75 m
Maximum Efficiency at 1100 RPM: 7.06% at 6.80 L/min, Head = 0.65 m

3.6 Experimental Phase

3.6.1 PIV Setup

The main components of the PIV system consisted of the following components:

- 100mW Laser for Illumination
- Cylindrical Lens for Planar Laser sheet
- Digital Camera for Image and Video Capture

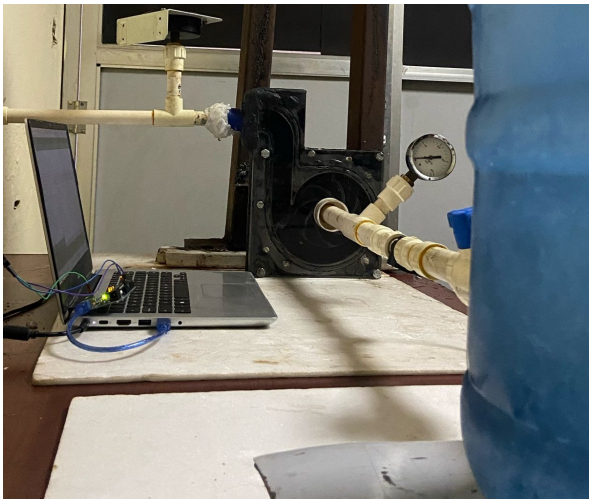

((a)) Experimental setup(Front View)

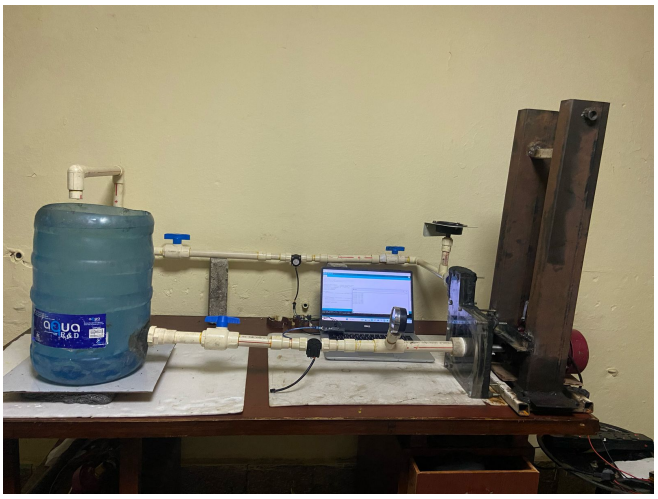

((b)) Experimental setup(Side View)

Figure 3.19: Fabricated Experimental Setup

Figure 3.20: PIV Setup for Flow Visualization

- PIVLab for Velocimetry

3.6.2 PIV Validation

PIV was carried out on a flow channel consisting of a sinusoidal waveform structure in the channel shown in Fig. 3.23. The following flow and geometric conditions were set:

- Flow Velocity = 0.01 m/s
- Reynolds Number = 6000
- Peak-to-Peak = 60 mm
- Peak-to-Trough = 15 mm

((a)) Sony A6000

((b)) Chronos high-speed camera

Figure 3.21: Digital Cameras used for PIV

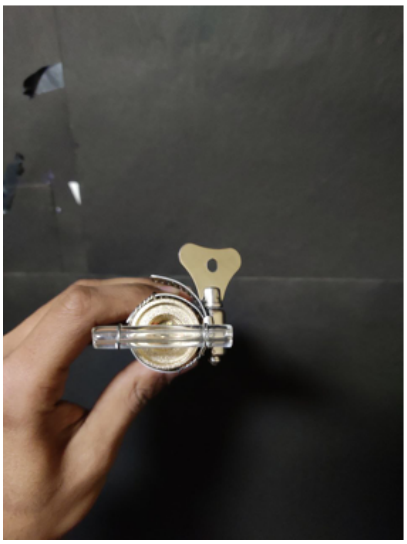

((a)) Front View

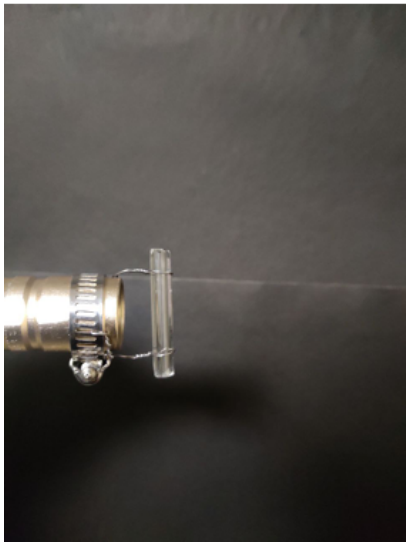

((b)) Side View

Figure 3.22: 100mW Laser and Cylindrical Lens used for Planar Illumination[6]

- Channel Length = 615 *mm*
- Channel width = 15 *mm*

The Sony A6000 digital camera was used to capture video of flow under the aforementioned conditions. A region of interest was selected to eliminate unnecessary computations, and the masking feature of PIVLab was used to mask the sinusoidal structure. The following filter settings were used for pre-processing of the obtained media:

- CLAHE with a window size of 64px
- High Pass with kernel size 15px
- Weiner2 denoise and low pass with window size 3px
- Subtraction of mean intensity

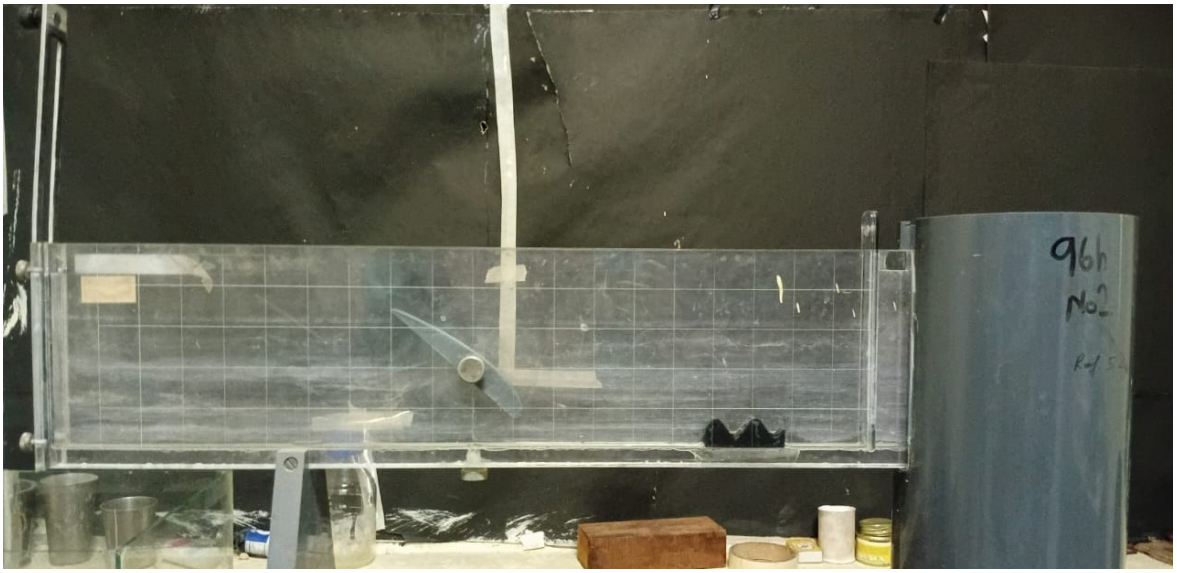

Figure 3.23: Flow Channel with Sinusoidal waveform Structure

This was followed by Multipass FFT cross-correlation under the following settings:

- Interrogation window size: $64px * 64px$
- Step Size: $16px$
- Pass 2: $32px$

It was seen that flow separation occurred at crests, followed by recirculation with a velocity minimum at the centre of recirculation as observed in Fig. 3.24(a). Vorticity was maximum at areas close to the crest where flow separation starts as observed in 3.24(b).

3.6.3 Flow Visualization of Centrifugal Pump Impeller using PIV

Volute of the pump and the impeller blade were illuminated with the LASER and the camera fixed at a position. The cameras used for the experiment are shown in Figure 3.21. This window size was selected to include 8-10 seeding particles per interrogation window. The images captured by the high speed camera could not produce meaningful results as the illumination of the seeding particles were not enough for the PIVlab software to analyze. Hence, Sony A6000 camera was used to capture the images of the impeller rotating at 10rpm and 30rpm. The motor speed was varied using the variable RPM controller and the speed was measured using tachometer. The pump was rotated clockwise as designed, and then it was rotated anticlockwise against the design specification. The direction of the motor was changed by swapping the wire inside the motor to change the polarity. The images obtained were pre-processed using the following filter settings:

- CLAHE with a window size of $64px$
- High Pass with kernel size $15px$
- Weiner2 denoise and low pass with window size $3px$
- Subtraction of mean intensity

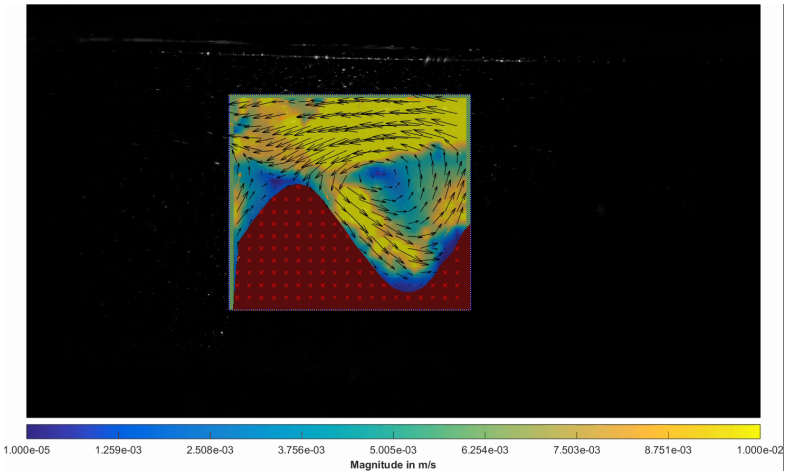

((a)) Velocity field-Sinusoidal Structure

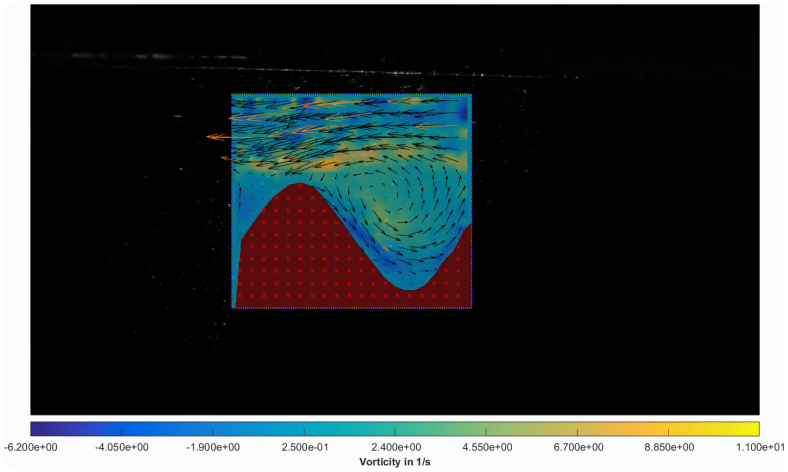

((b)) Vorticity field-Sinusoidal Structure

Figure 3.24: Velocity and vorticity fields at a certain time in the sine wave.

Masking feature of PIVLab was used to mask the blade and under-illuminated region of the image to obtain a region of interest focused on the volute section immediately outside the impeller. The images were then analyzed using following correlation settings:

- Single pass FFT Cross-Correlation
- Interrogation window size: $64px * 64px$
- Step Size: $32px$
- Pass 2: $32px$

The frames extracted by PIVlab were calibrated by measuring the width of the impeller blade to get the results.

CHAPTER 4
RESULT AND DISCUSSION

4.1 Result

4.1.1 Flow Visualization in centrifugal pump impeller and volute

The post-processed images of the mean velocity vectors of the flow in the volute just outside the impeller showing the variation in vorticity, for the motor running at 30 rpm in the intended clockwise direction is shown in Figure 4.1. The flow rate was 0 and the input head was 0.2m.

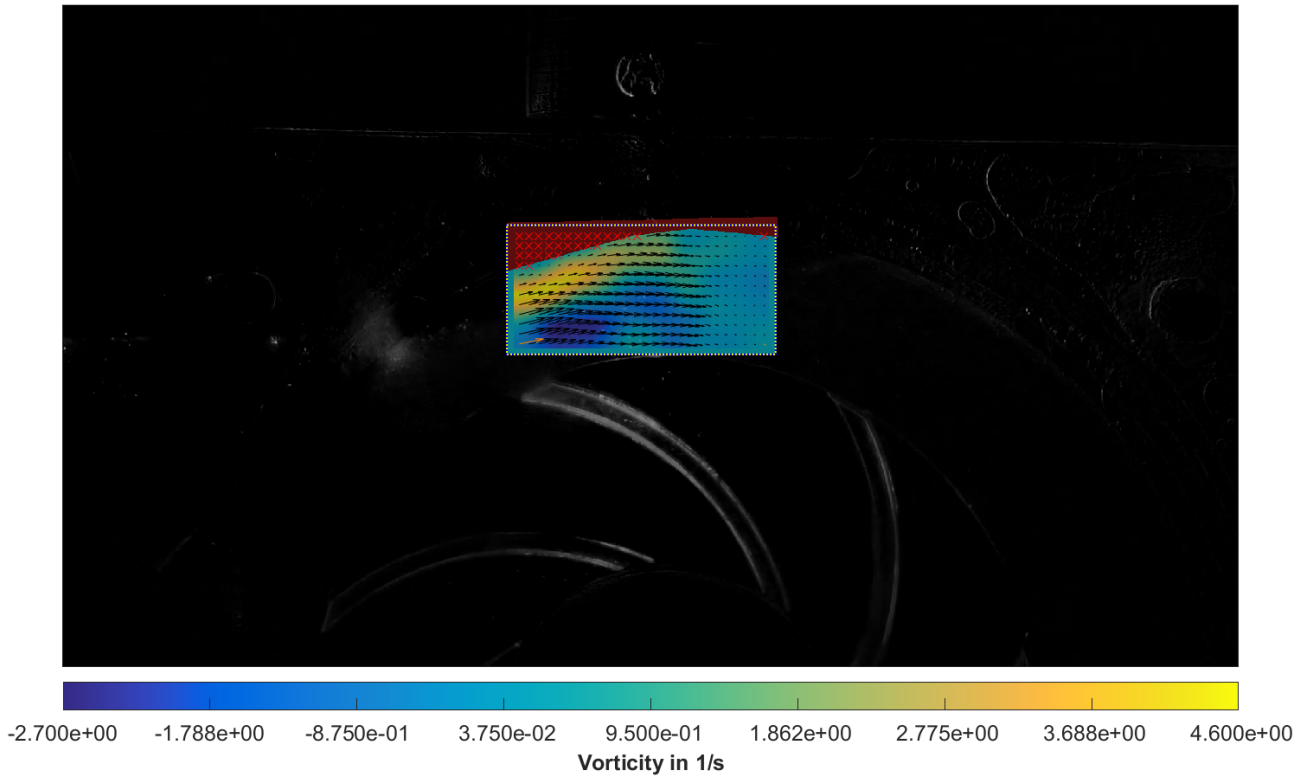

Figure 4.1: Mean velocity vectors of flow at 30rpm in clockwise direction showing variation in vorticity

We can see that the flow near the impeller closely follows the impeller blade in clockwise direction. However, the flow further from the impeller takes time to adjust, creating flow in opposite direction. This delay can lead to the formation of vortices. A polyline was drawn from the impeller to the volute, and the vorticity data was extracted.
The flow near the impeller is in the direction of the impeller as the vorticity is negative (clockwise direction).As we move away from the impeller, the vorticity changes towards positive, meaning in anti-clokwise direction. This may create a condition for the formation of vortices. This phenomenon was greatly magnified when the impeller rotated in the anticlockwise direction, as we can see in Figure 4.3.
Vortex formation was more pronounced when the motor operated in the anticlockwise direction, as confirmed by the streamlines drawn to validate the findings. The flow near the impeller followed the blade's motion in an anti-clockwise direction, while the flow farther away remained inactive, leading to the formation of vortex. This can be seen through data extracted from a polyline drawn from impeller to the volute as shown in Figure 4.4.

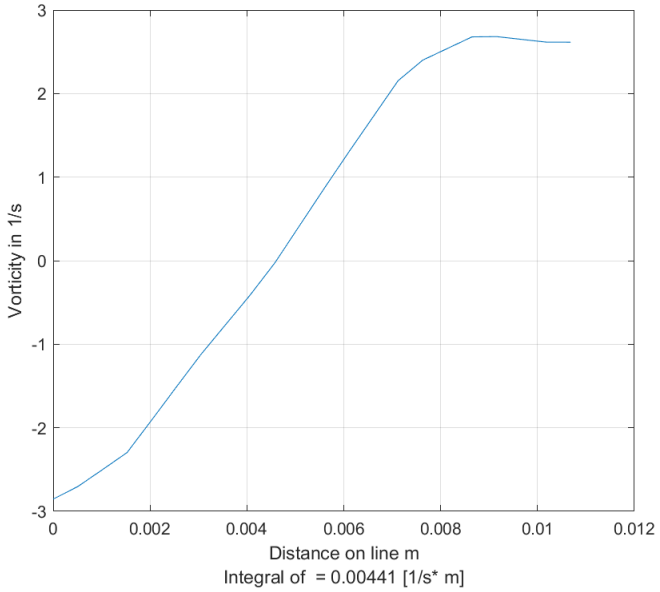

Figure 4.2: Variation in vorticity from impeller to the volute

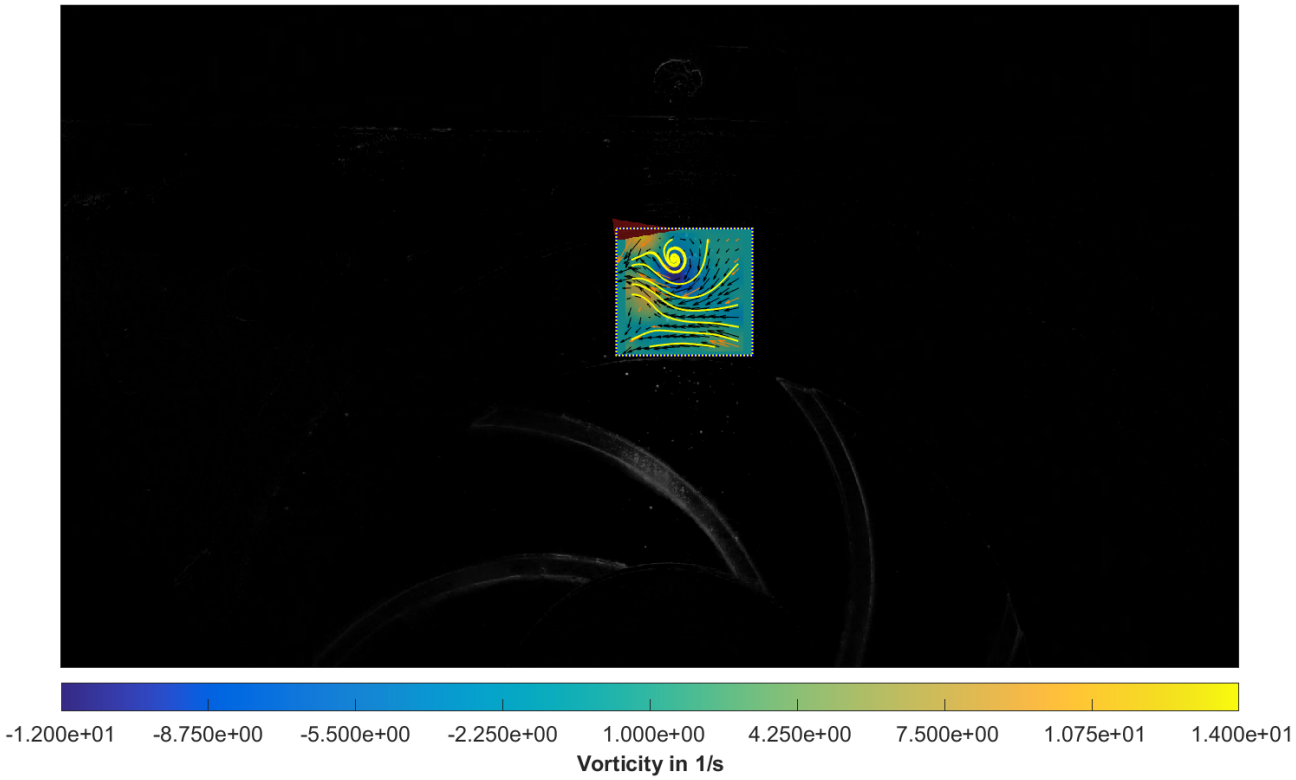

Figure 4.3: Variation in vorticity and streamlines to visualize it

Here, the flow near the impeller followed the impeller's anticlockwise direction showing positive vorticity. As we moved further away from the impeller the magnitude of vorticity reached the maximum at a negative value, showing the flow in the clockwise direction. This caused vortex formation as seen through the streamlines. The flow still further away was not affected yet during the time of observation, and the vorticity tended to go closer to 0.
The experiment was futher conducted at the pump rotating at 10 rpm in anticlockwise direction. Similar phenomenon could be seen as shown in the Figure 4.5.

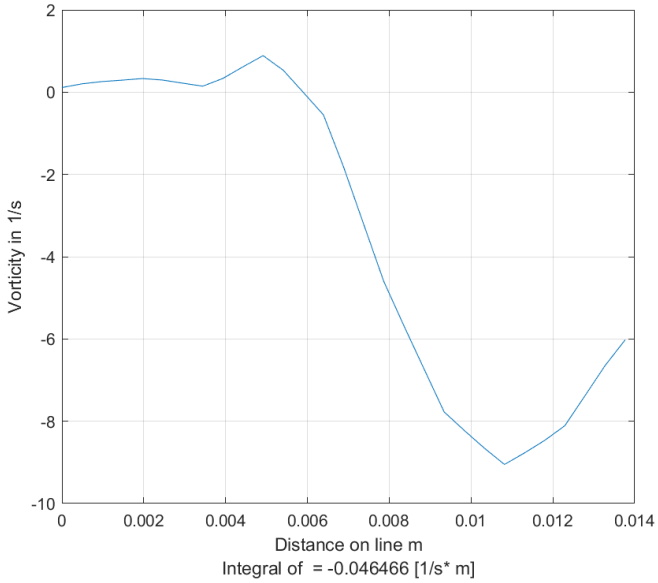

Figure 4.4: Variation in vorticity and streamlines to visualize it

Polyline was drawn through the impeller to the volute, and the variation in vorticity was noted as showin in Figure 4.6.
Flow near the impeller followed the impeller in anticlockwise direction showing positive vorticity, and the flow further away from the impeller tended to clockwise direction, which is opposite from the direction of the impeller.

4.2 Limitations

Although this study demonstrates the potential of the particle image velocimetry(PIV) technique in flow visualization in complex structures and machines, the limitation must be acknowledged.

1. The availability of a high end equipment such as high intensity laser for high-speed camera and optical system that could concentrate the intensity of laser in a plane, were limited. This limited the accuracy of PIV results in high-speed flow regions of the pump. Hence, the results obtained in this study is limited to very low speed condition of the impeller.

4.3 Problems Faced

During the course of this study, several challenges were encountered that impacted the results and outcome. The problems faced are outlined below:

1. The accuracy of Particle Image Velocimetry (PIV) post-processing is highly dependent on the quality of the captured images and videos, which, in turn, relies on the performance of the laser,camera and the optical systems. Acquiring the high end systems posed technical and financial difficulties.

2. The fabrication and assembly of the pump introduced permanent marks and spots on the filmed region, leading to unwanted background noise in the captured images. This interference distorted the PIV analysis, causing deviations from the actual flow measurements and affecting the accuracy of the results.

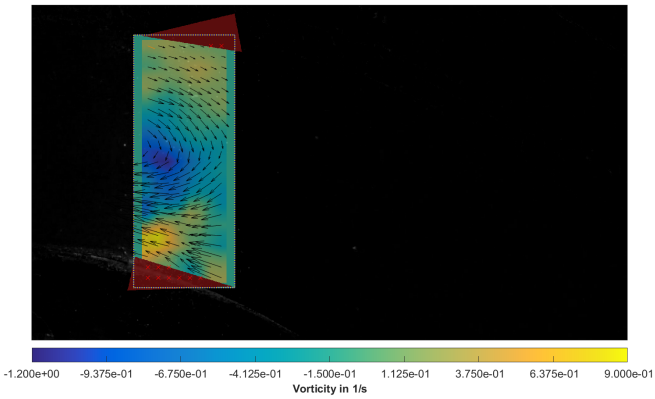

((a)) Variation in vorticity in mean velocity vectors of impeller running at 10 rpm

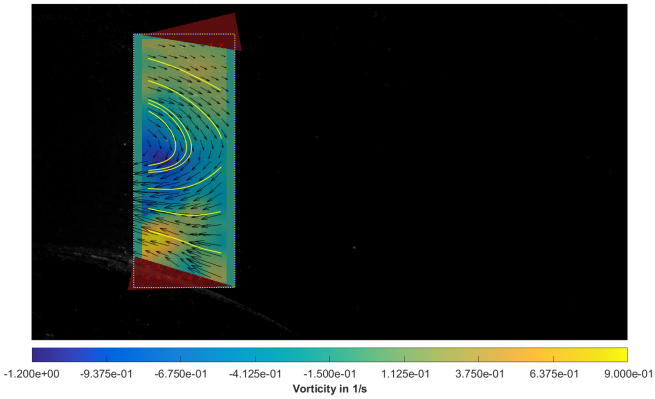

((b)) Streamlines showing the direction of flow in mean velocity field of impeller running at 10 rpm

Figure 4.5: Post processed images of pump running at 10 rpm

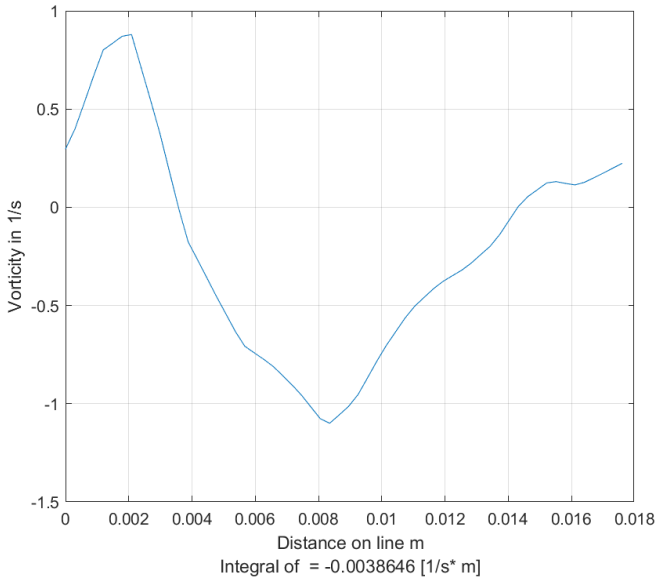

Figure 4.6: Variation in vorticity from impeller to the volute in impeller running at 10rpm anticlockwise

3. Leakages from the pump casing created significant challenges in conducting the experiment efficiently.

4. The proper aligning of shaft, motor and the impeller caused significant difficulties.

4.4 Budget Analysis

The Budget for the overall project is shown in Table 4.1

Table 4.1: Budget Analysis

S.N.	Particulars	Rate (Rs.)	Quantity	Cost (Rs.)
1	UV glue	1500/-	1	1500
2	Acrylic Sheets	-	-	5150
3	NUMMAKERS PLA+ 3D filament	2810/-	1	2810
4	6204 Bearing MGF	320/-	4	1280
5	Pipe and fittings	-	-	4915
6	RPM Controller	850/-	2	1700
7	Pressure Gauge	850/-	2	1700
8	Lathe Machining	-	-	2350
9	Nylon Rod (for Bushing)	900/-	1	900
10	Aluminium Rod (for Shaft)	1070/-	1	1070
11	Nut, Bolts, Washers, Allen Key	-	-	925
12	Glass Tank	1500/-	1	1500
13	Pump Fabrication	-	-	5000
	Total			30800

4.5 Discussion

The analysis of flow behavior in the centrifugal pump at low 10 rpm and 30 rpm, showed the velocity profiles and vorticity. The flow near the impeller followed the direction of the impeller, while the flow away from the impeller took some time to adjust. This created the condition for the formation of vortex. The effect was magnified when the pump was run in the off-design, anti-clockwise direction, where we could see vortex formation clearly. This was confirmed through streamline visualization, which validated the flow patterns and highlighted regions of strong rotational motion. The delayed response of the flow away from the impeller results in localized regions of recirculation, intensifying vortex formation. The presence of vortices can have significant implications in practical applications. Excessive vortex generation may introduce unwanted turbulence, energy losses, or uneven mixing. Understanding these effects is crucial in optimizing impeller design and operational parameters for specific industrial applications.

Due to resource limitations, the experiment was conducted at low RPM, and at 0 flow rate restricting the ability to analyze flow behavior at the higher RPMs at which the pump typically operates. As a result, the practical implications of vortex formation under real operating conditions could not be fully considered. Higher rotational speeds may influence the intensity and stability of vortex structures, potentially altering the overall flow characteristics.

CHAPTER 5
CONCLUSION AND FUTURE ENHANCEMENT

5.1 Conclusion

This study focused on flow visualization technique of Particle Image Velocimetry (PIV), and flow was visualized in the impeller and volute of centrifugal pump, where velocity fields and vorticity variations were extracted. The pump was run at low rpms, and in clockwise and anticlockwise direction. Videos were taken for PIV in these conditions and cross-correlation technique was implemented in post-processing with the help of PIVlab software.

The centrifugal pump was designed with a detailed CAD model, and fabricated using precision laser cutting of transparent acrylic sheets. The pump was assembled, and a closed loop water intake and exit system was constructed with reservoir and pipe fittings. Flow rate and head were measured and pump curve was developed with Best Efficiency Point (BEP). The outcome of this study will contribute to a better understanding of the internal flow dynamics within a centrifugal pump, particularly in relation to vortex formation.

Along with experiments, a simulation phase was also carried out to predict the pump's performance. The simulation gave an efficiency of 47.49%, while the theoretical efficiency was 54.21%. In comparison, the actual efficiency of the fabricated pump was much lower at 7.22%, mainly because of losses like leakage, friction, and fabrication imperfections. Even with these challenges, the study successfully captured important flow features and pointed out areas where design improvements could be made.

5.2 Scope for Future Enhancement

The project provides valuable insights on the technique of Particle Image Velocimetry(PIV) for flow visualization of various phenomenon such as turbulence and the flow of water in centrifugal pump. There are still many enhancements that can be done in the future to improve the accuracy and application of the findings.

- **Higher resolution imaging:** With a laser with higher intensity and equipped with better optical system, the images can be captured at very high resolution with high speed camera, which will provide the ideal quality images for post-processing of the image, that could provide more accurate results.
- **Study of Cavitation:** Future enhancement could include the study of cavitation and its effects in the centrifugal pump impeller.
- **Multi-phase fluid study:** This project focused solely on single phase fluid flow, but multi-phase flow is an exciting and emerging field that can be investigated in the future.

REFERENCES

[1] A. Stepanoff, *Centrifugal and Axial Flow Pumps: Theory, Design, and Application*. Krieger Publishing Company, 1993.

[2] R. M. Perissinotto, R. F. Cerqueira, W. D. Fonseca, W. M. Verde, J. L. Biazussi, A. C. Bannwart, E. M. Franklin, and M. S. Castro, "Particle image velocimetry in a centrifugal pump: Details of the fluid flow at different operation conditions," *Flow Measurement and Instrumentation*, vol. 89, p. 102282, 2023.

[3] W. Thielicke and E. J. Stamhuis, "Pivlab – towards user-friendly, affordable and accurate digital particle image velocimetry in matlab," *Journal of Open Research Software*, vol. 2, 10 2014.

[4] D. Wulff, "Piv measurements in pumps," 2006.

[5] R. M. Perissinotto, W. D. Fonseca, R. F. Cerqueira, W. M. Verde, J. L. Biazussi, E. M. Franklin, A. C. Bannwart, and M. S. Castro, "Flow visualization in the impeller and diffuser of a centrifugal pump using time-resolved particle image velocimetry,"

[6] K. C. Devkota, P. Mishra, S. Adhikari, and S. Banjade, "Experimental investigation of flow over a cylinder and wing with vortex generators using piv," bachelor's thesis, Tribhuvan University Institute of Engineering, Pulchowk Campus, 2024.

[7] W. Monte Verde, *Performance modeling of ESP pumps performance operating with gas-viscous liquid mixtures*. PhD thesis, University of Campinas Brazil, 2016.

[8] R. M. Perissinotto, W. M. Verde, J. L. Biazussi, N. A. V. Bulgarelli, W. D. P. Fonseca, M. S. de Castro, E. de Moraes Franklin, and A. C. Bannwart, "Flow visualization in centrifugal pumps: A review of methods and experimental studies," *Journal of Petroleum Science and Engineering*, vol. 203, p. 108582, 2021.

[9] M. Raffel, C. Willert, S. Wereley, and J. Kompenhans, *Particle Image Velocimetry: A Practical Guide*. 01 2007.

[10] A. Ciocanea, S. Budea, and I.-A. Șișman, "Improving the hydraulic efficiency of centrifugal impellers by using reverse engineering — case study of a centrifugal pump," pp. 428–431, 10 2017.

[11] G. Dhungana, S. Gautam, and Y. Karki, "Fabrication of particle image velocimetry setup for experimentation at low reynolds number," bachelor's thesis, Tribhuvan University Institute of Engineering, Pulchowk Campus, 2023.

[12] N. Pedersen, "Experimental investigation of flow structures in a centrifugal pump impeller using particle image velocimetry," 2001.

[13] R. Perissinotto, W. Fonseca, R. Cerqueira, W. Monte Verde, J. Biazussi, M. Castro, and A. Bannwart, "Development of a transparent pump prototype for flow visualization purposes," in *Proceedings of Rio Oil & Gas Expo and Conference*, pp. 26–29, Brazilian Petroleum and Gas Institute, 2022.

Appendices

APPENDIX A
FABRICATION

((a)) Fabricated acrylic parts (before assembly)

((b)) Adhesive (UV glue)

((c)) Volute fabrication

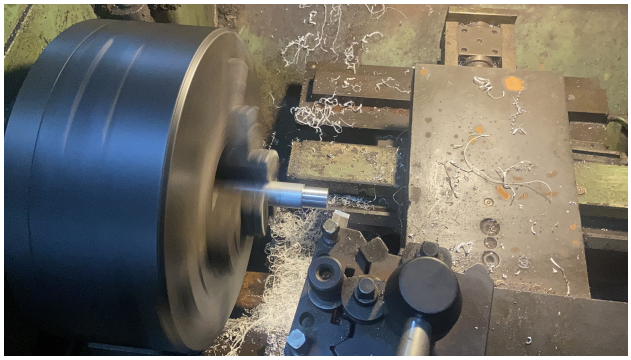

((d)) Shaft fabrication

Figure A.1: Fabrication process components: (a) acrylic parts before assembly, (b) UV adhesive, (c) volute fabrication, and (d) shaft fabrication

APPENDIX B
CODES

B.1 Arduino Code: Flow sensor

```
volatile int flow_frequency;  // Measures flow sensor pulses
float flow_rate;  // Calculated litres per minute (L/min)
const unsigned char flowsensor = 2;  // Sensor Input
unsigned long currentTime;
unsigned long cloopTime;

void flow()
{
    flow_frequency++;//Increase pulse count every time a pulse is detected
}

void setup()
{
pinMode(flowsensor, INPUT_PULLUP);  // Use internal pull-up resistor
Serial.begin(9600);
attachInterrupt(digitalPinToInterrupt(flowsensor),flow, RISING);
//Setup Interrupt
currentTime = millis();
cloopTime = currentTime;
}

void loop()
{
    currentTime = millis();

    // Every second, calculate and print litres/minute
    if (currentTime >= (cloopTime + 1000))
    {
        cloopTime = currentTime;  // Updates cloopTime
        flow_rate = (flow_frequency / 7.5);  // Convert pulses to L/min
        flow_frequency = 0;  // Reset pulse counter

        Serial.print("Flow Rate: ");
        Serial.print(flow_rate, 2);  // Print with 2 decimal places
        Serial.println(" L/min");
    }
}
```

APPENDIX C
CODES

C.1 Matlab Code to Generate Theoretical Head Curve

```
%% Pump Performance Analysis - Dual Speed
% Common Parameters
d2 = 109e-3;        % Outlet diameter [m]
beta2_deg = 46.8;   % Blade angle at outlet [°]
b2 = 6e-3;          % Blade height [m]
t = 5.5e-3;         % Blade thickness [m]
Z = 7;              % Number of blades
g = 9.81;           % Gravity [m/s²]
rho = 1000;         % Water density [kg/m³]

% 1000 RPM Configuration
N1 = 1000;
P_input1 = 7.69439;     % Input power [W]
Q_max_lpm1 = 6.8;       % Max flow rate [L/min]

% 1100 RPM Configuration
N2 = 1100;
P_input2 = 10.241238;   % Input power [W]
Q_max_lpm2 = 7.2;       % Max flow rate [L/min]

%% Calculations for Both Speeds
% Initialize function handles for calculations
calculatePerformance = @(N, P_input, Q_max_lpm) struct(...
    'N', N, ...
    'Q_plot', linspace(0, Q_max_lpm, 200), ... % Flow in L/min
    'H', [], 'eta', [], 'phi', [], 'psi', []);

% 1000 RPM Calculations
config1 = calculatePerformance(N1, P_input1, Q_max_lpm1);
Q_max1 = config1.Q_plot(end) / (1000*60); % Convert L/min to m³/s
beta2 = deg2rad(beta2_deg);
u2_1 = pi * d2 * N1 / 60;
A2_1 = (pi * d2 - Z * t) * b2;
Q1 = linspace(0, Q_max1, 200);
v_m2_1 = Q1 / A2_1;
v_u2_1 = u2_1 - (v_m2_1 ./ tan(beta2));
config1.H = (u2_1 .* v_u2_1) / g;
config1.eta = (rho * g * Q1 .* config1.H / P_input1) * 100;
config1.phi = Q1 / (A2_1 * u2_1);
config1.psi = (g * config1.H) / u2_1^2;

% 1100 RPM Calculations
```

```
config2 = calculatePerformance(N2, P_input2, Q_max_lpm2);
Q_max2 = config2.Q_plot(end) / (1000*60); % Convert L/min to m³/s
u2_2 = pi * d2 * N2 / 60;
A2_2 = (pi * d2 - Z * t) * b2;
Q2 = linspace(0, Q_max2, 200);
v_m2_2 = Q2 / A2_2;
v_u2_2 = u2_2 - (v_m2_2 ./ tan(beta2));
config2.H = (u2_2 .* v_u2_2) / g;
config2.eta = (rho * g * Q2 .* config2.H / P_input2) * 100;
config2.phi = Q2 / (A2_2 * u2_2);
config2.psi = (g * config2.H) / u2_2^2;

%% Generate Plots for Both Speeds
% 1000 RPM Plots
figure(1);
yyaxis left;
plot(config1.Q_plot, config1.H, 'b-', 'LineWidth', 2);
ylabel('Head (m)', 'FontSize', 12);
ylim([3.25 3.35]);
yyaxis right;
plot(config1.Q_plot, config1.eta, 'r--', 'LineWidth', 1.5);
ylabel('Efficiency (%)', 'FontSize', 12);
xlabel('Flow Rate (L/min)', 'FontSize', 12);
title('1000 RPM: Head & Efficiency vs Flow', 'FontSize', 14);
legend('Head', 'Efficiency', 'Location', 'northeast');
grid on;

figure(2);
plot(config1.phi, config1.psi, 'k-', 'LineWidth', 1.5);
hold on;
plot(config1.phi, config1.eta, 'm--', 'LineWidth', 1.5);
title('1000 RPM: Dimensionless Coefficients', 'FontSize', 14);
xlabel('\Phi', 'FontSize', 12);
ylabel('\Psi / Efficiency (%)', 'FontSize', 12);
legend('Head Coefficient (\Psi)', 'Efficiency', 'Location', 'southwest');
grid on;

% 1100 RPM Plots
figure(3);
yyaxis left;
plot(config2.Q_plot, config2.H, 'g-', 'LineWidth', 2);
ylabel('Head (m)', 'FontSize', 12);
ylim([3.95 4.05]);
yyaxis right;
plot(config2.Q_plot, config2.eta, 'm--', 'LineWidth', 1.5);
ylabel('Efficiency (%)', 'FontSize', 12);
xlabel('Flow Rate (L/min)', 'FontSize', 12);
title('1100 RPM: Head & Efficiency vs Flow', 'FontSize', 14);
```

```
legend('Head', 'Efficiency', 'Location', 'northeast');
grid on;

figure(4);
plot(config2.phi, config2.psi, 'b-', 'LineWidth', 1.5);
hold on;
plot(config2.phi, config2.eta, 'r--', 'LineWidth', 1.5);
title('1100 RPM: Dimensionless Coefficients', 'FontSize', 14);
xlabel('\Phi', 'FontSize', 12);
ylabel('\Psi / Efficiency (%)', 'FontSize', 12);
legend('Head Coefficient (\Psi)', 'Efficiency', 'Location', 'southwest');
grid on;

%% Numerical Outputs
fprintf('1000 RPM Performance Summary:\n');
disp(table(config1.Q_plot', config1.H', config1.eta', ...
    'VariableNames', {'Flow_LPM', 'Head_m', 'Efficiency_%'}));

fprintf('\n1100 RPM Performance Summary:\n');
disp(table(config2.Q_plot', config2.H', config2.eta', ...
    'VariableNames', {'Flow_LPM', 'Head_m', 'Efficiency_%'}));
```

C.2 Matlab Code to Generate Actual Pump Head Curve

```
% Pump data for two speeds
flow_1100 = [0, 0.3, 0.53, 1.6, 2.8, 3.6, 4.8, 5.33,...
             6, 6.8, 7, 7.2]; % l/min (1100 RPM)
head_1100 = [1.4, 1.4, 1.3, 1.2, 1, 0.9, 0.8, 0.75,...
             0.7, 0.65, 0.6, 0.5]; % m (1100 RPM)

flow_1000 = [0, 0.5, 1.5, 1.73, 2.27, 3, 3.07, 3.73,...
             4, 4.13, 4.27, 4.93, 5.07, 5.6, 6, 6.8]; % l/min
head_1000 = [1.2, 1.2, 0.95, 0.95, 0.9, 0.85, 0.85,...
             0.85, 0.8, 0.8, 0.75, 0.75, 0.7, 0.65, 0.6, 0.5]; % m

% Power inputs
P_input_1000 = 7.69439;   % 1000 RPM (W)
P_input_1100 = 10.241238; % 1100 RPM (W)
rho = 1000; g = 9.81;

% Efficiency calculation
calculateEfficiency = @(Q, H, P_input) ...
    (Q/60000 .* H * rho * g / P_input) * 100;
eff_1100 = calculateEfficiency(flow_1100, head_1100, P_input_1100);
eff_1000 = calculateEfficiency(flow_1000, head_1000, P_input_1000);

%% Generate Plots
% 1100 RPM Plot
```

```
figure(1);
flow_cont = linspace(min(flow_1100), max(flow_1100), 1000);
head_cont = interp1(flow_1100, head_1100, flow_cont, 'pchip');
eff_cont = interp1(flow_1100, eff_1100, flow_cont, 'pchip');

yyaxis left;
plot(flow_cont, head_cont, 'b-', flow_1100, head_1100, 'bo',...
    'MarkerFaceColor', 'b');
ylabel('Head (m)', 'FontSize', 12);
ylim([0 1.5]);
yyaxis right;
plot(flow_cont, eff_cont, 'r--', flow_1100, eff_1100, 'rs',...
    'MarkerFaceColor', 'r');
ylabel('Efficiency (\%)', 'FontSize', 12);
title('1100 RPM: Head \& Efficiency (P_{in}=10.24W)',...
    'FontSize', 14);
xlabel('Flow Rate (l/min)', 'FontSize', 12);
legend('Head (Interp.)', 'Head (Data)', 'Efficiency (Interp.)',...
    'Efficiency (Data)', 'Location', 'Best');
grid on;

% 1000 RPM Plot
figure(2);
flow_cont = linspace(min(flow_1000), max(flow_1000), 1000);
head_cont = interp1(flow_1000, head_1000, flow_cont, 'pchip');
eff_cont = interp1(flow_1000, eff_1000, flow_cont, 'pchip');

yyaxis left;
plot(flow_cont, head_cont, 'b-', flow_1000, head_1000, 'bo',...
    'MarkerFaceColor', 'b');
ylabel('Head (m)', 'FontSize', 12);
ylim([0 1.5]);
yyaxis right;
plot(flow_cont, eff_cont, 'r--', flow_1000, eff_1000, 'rs',...
    'MarkerFaceColor', 'r');
ylabel('Efficiency (\%)', 'FontSize', 12);
title('1000 RPM: Head \& Efficiency (P_{in}=7.69W)',...
    'FontSize', 14);
xlabel('Flow Rate (l/min)', 'FontSize', 12);
legend('Head (Interp.)', 'Head (Data)', 'Efficiency (Interp.)',...
    'Efficiency (Data)', 'Location', 'Best');
grid on;

%% Numerical Output
% 1100 RPM Data
fprintf('1100 RPM Performance (P_{input}=10.24W):\n');
T1100 = table(flow_1100', head_1100', eff_1100',...
    'VariableNames', {'Flow_l_min','Head_m','Efficiency_%'});
```

```
disp(T1100);
[~, idx] = max(eff_1100);
fprintf('Max Efficiency: %.2f%% at %.2f L/min, Head=%.2f m\n\n',...
    eff_1100(idx), flow_1100(idx), head_1100(idx));

% 1000 RPM Data
fprintf('1000 RPM Performance (P_{input}=7.69W):\n');
T1000 = table(flow_1000', head_1000', eff_1000',...
    'VariableNames', {'Flow_l_min','Head_m','Efficiency_%'});
disp(T1000);
[~, idx] = max(eff_1000);
fprintf('Max Efficiency: %.2f%% at %.2f L/min, Head=%.2f m\n',...
    eff_1000(idx), flow_1000(idx), head_1000(idx));
```

APPENDIX D
CAD DRAWING OF PUMP COMPONENTS

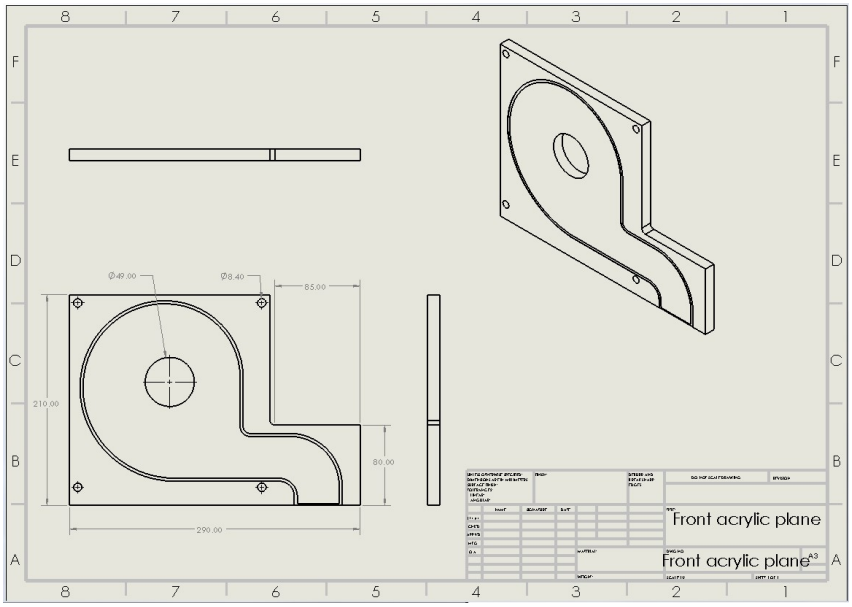

Figure D.1: Front Plane

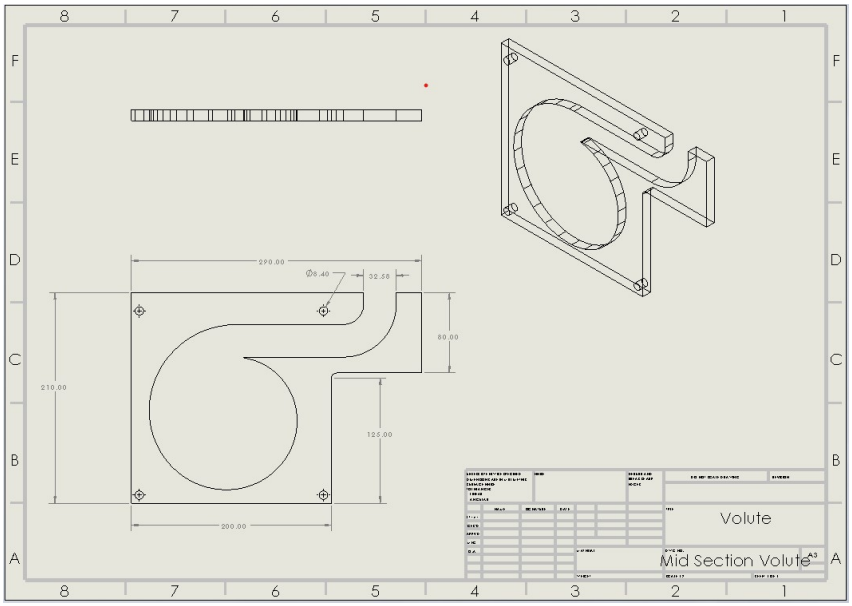

Figure D.2: Mid Section Volute

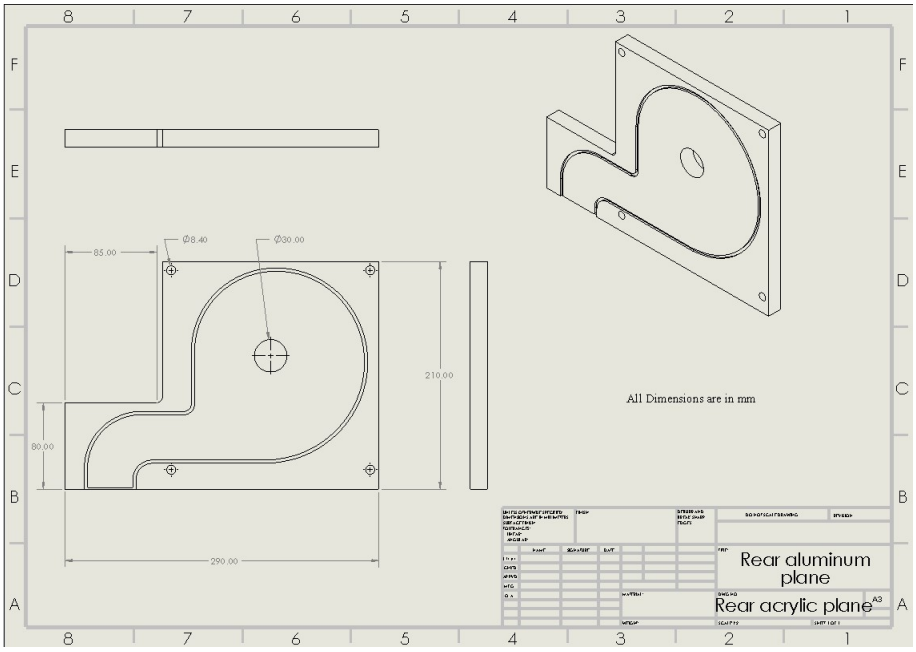

Figure D.3: Rear Acrylic Plane

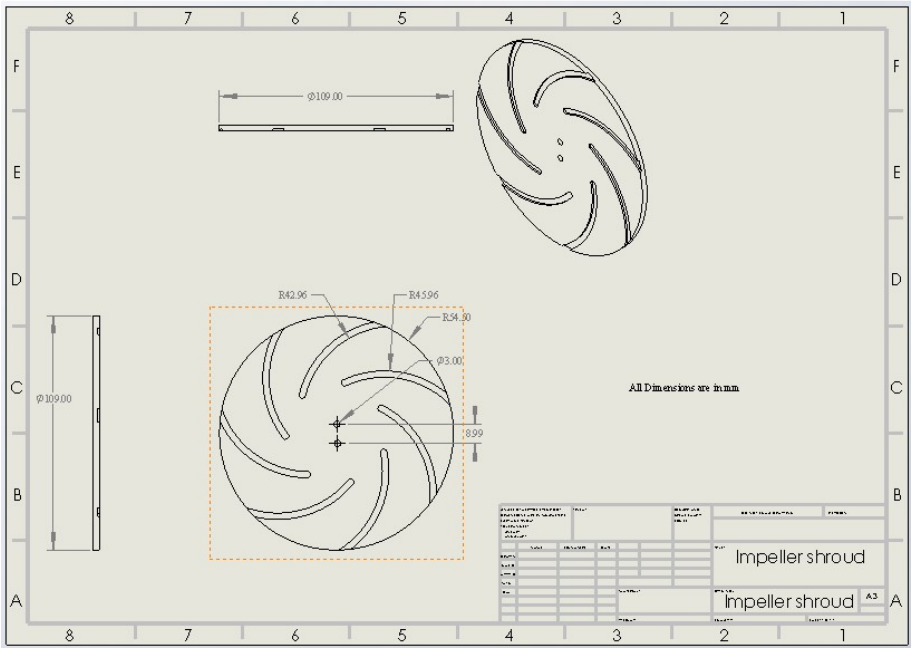

Figure D.4: Impeller Shroud

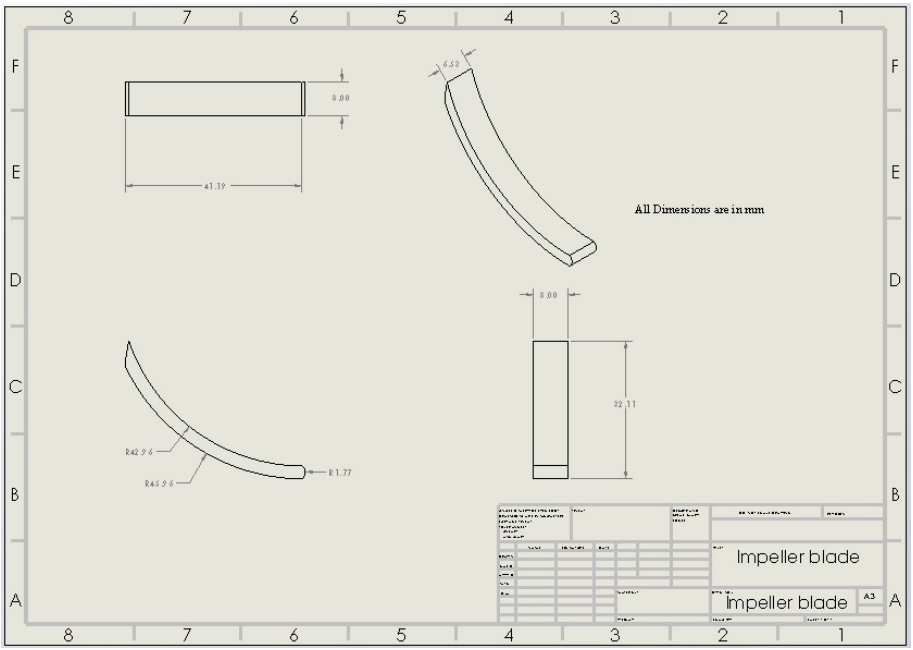

Figure D.5: Impeller Blade

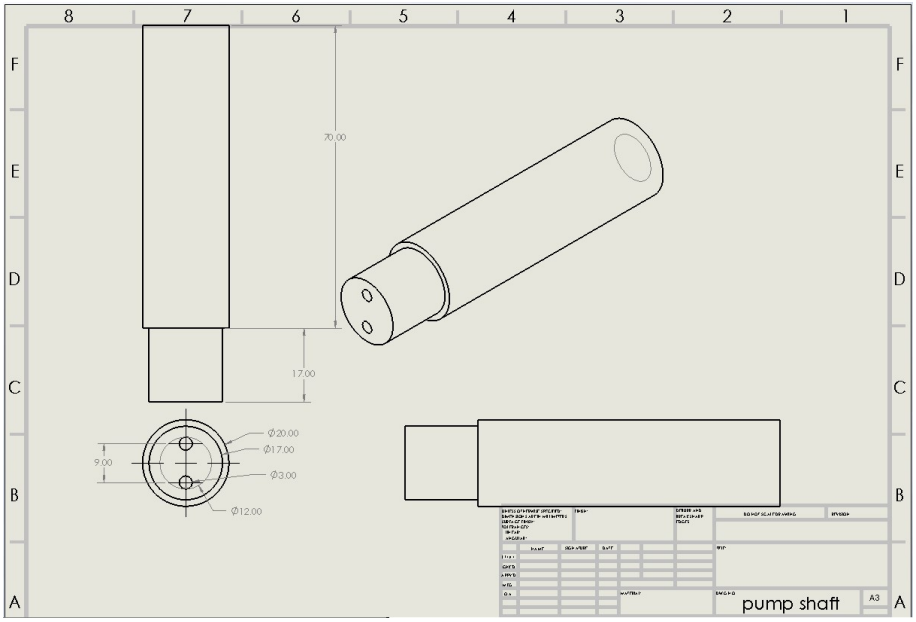

Figure D.6: Pump Shaft